Geoelectrical Characterization of Sulphate Rocks

Ander Guinea Maysounave

Programa de Doctorat de Ciències de la Terra

GEOELECTRICAL CHARACTERIZATION OF SULPHATE ROCKS

Ander Guinea Maysounave

2011

Advisors / Directors de tesi:

Drs. Elisabet Playà Pous & Lluís Rivero Marginedas

Departament de Geoquímica, Petrologia i Prospecció Geològica

UNIVERSITAT DE BARCELONA

Electrical Properties of Sulphates

Ander Guinea 2011

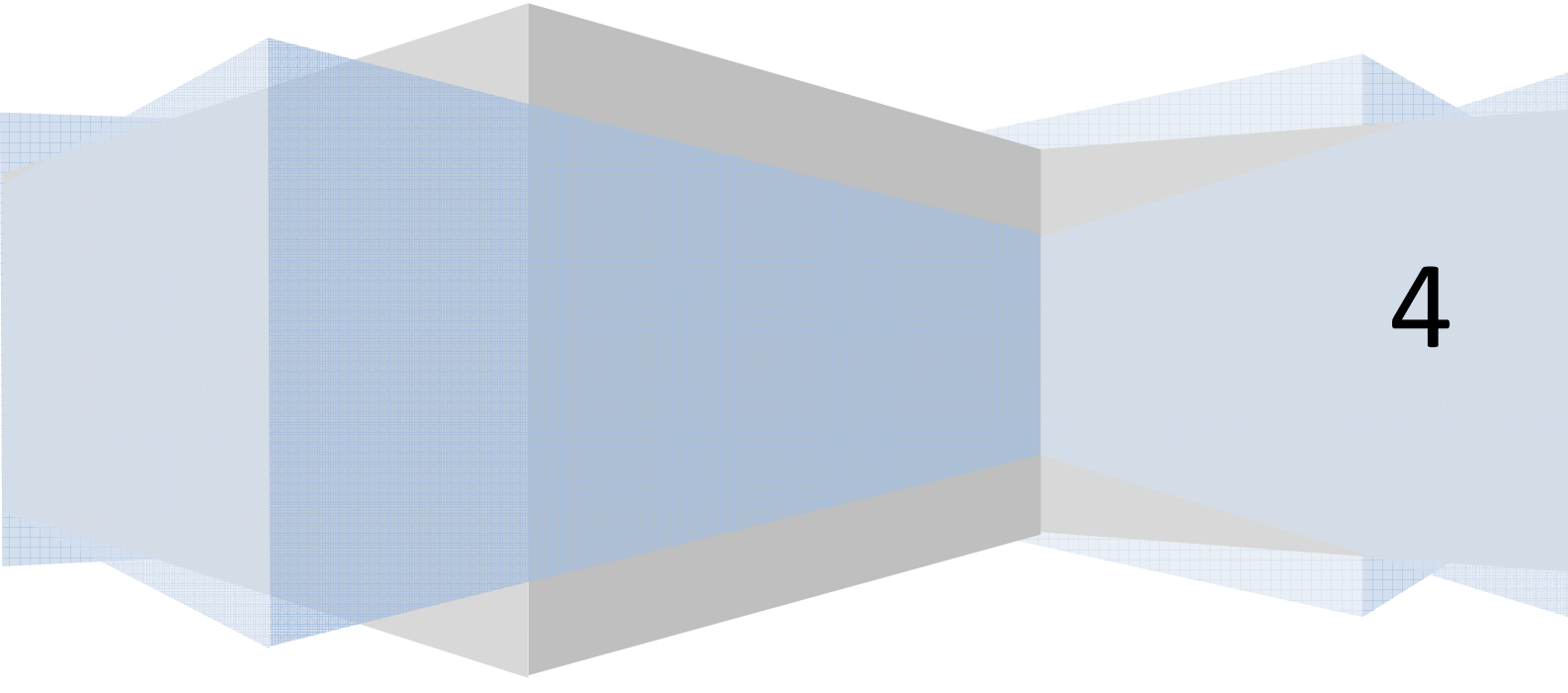

4

.1 GYPSUM

.1.1 Introduction:

Gypsum is made of calcium sulphate with two water molecules ($CaSO_4 \cdot 2H_2O$). It can be found in the nature as primary gypsum (forming selenite crystals or gypsarenite deposits) or as secondary gypsum, coming from the hydration of anhydrite ($CaSO_4$) (displaying alabastrine, megacristalline or porfiroblastic textures). Principal sulphate rocks (gypsum, anhydrite, glauberite and thenardite) are currently exploited with economical interest. Gypsum rocks are mainly constituted by gypsum minerals with different amounts of anhydrite, clay minerals and carbonates (calcite and/or dolomite), among others. Evaporitic deposits are characterized for having heterogeneous nature both vertical and horizontally due to primary and secondary processes. Gypsum rocks are impervious so water cannot run along them (no primary porosity contained). In any case the presence of water can dissolve the deposits creating karst structures (secondary porosity).

More than $9x10^4$ tones of industrial gypsum are produced each year in the world. Gypsum is used in the construction sector as primary matter due to his binder property. Furthermore, gypsum is innocuous and has properties of acoustic absorption, thermal insulation and hygrometric regulation. The main gypsum producer countries are USA, Spain, Canada and Iran. To determine the potential economical interest of a gypsum deposit, the aspects to be studied are mainly: a) the thickness of the gypsum layer (a layer has to have at least a width of 1.6 meter to be rentable), b) the quantity of clay in the composition of the gypsum rock (it must be less than 20%) and c) the possible structures and discontinuities related to the deposit (due to the possible water filtration that can affect the extractive activity) (Bonetto et al. 2008).

Published geoelectrical resistivity values for gypsum oscillate between 10 and 1200 ohm.m (table 4.1). Nevertheless, the cause of the wide range of electrical resistivity value of gypsum has not been investigated and the relationship between the lutite and gypsum minerals has not been quantified. These values are higher than the assigned resistivity of lutites (about 1 to 100 ohm.m) (Orellana 1972). The measuring of chargeability in gypsum rocks has not been object of previous researches but the chargeability properties of clay have been widely studied (Takakura and Nakada 2006; Deucester and Kauffman 2009). Nevertheless, the range of chargeability values for clays has not been specifically determined given that many variables are involved (grain size, composition, measure time…). As a general

trend, the clay chargeability values are rather low than the chargeability anomalies given by the presence of metallic minerals.

REFERENCE	RESISTIVITY VALUE (ohm.m)	AUTHOR'S COMMENTS
Lugo et al. (2008)	80-1000	The lower values are related to the presence of lutites within the gypsum rocks. The higher values correspond to presence of anhydrite within gypsum.
Ball et al. (2006)	25-500 / 500-1000	The values are directly obtained from inverted geoelectrical profiles. There are two ranges of values depending on the porosity of gypsum.
Asfahani and Mohammad (2002)	24-1200	The values are measured by vertical electrical soundings in a gypsum and anhydrite formation.
Benson and Kaufmann (2001)	100-150 / >300	The lower range is considered for unconsolidated gypsum sediments. Unweathered gypsum has a value greater than 300 ohm.m.
Rider (1986)	1000	The values are obtained from measuring electrical resistivity by diagraphy system.
Orellana (1982)	10-1000	The lower values are related to marls. When gypsum is associated with anhydrite, the electrical resistivity value can overcome 1000 ohm.m.

Table 4.1: Published electrical resistivity values for gypsum rocks.

Gypsum deposits have been studied with geoelectrical methods; a direct relationship between the electrical resistivity values of the gypsum rocks and its lithological composition has been established, with the presence of lutites being the main controlling factor in the geoelectrical response of the deposit. A geoelectrical classification has been elaborated comparing the resistivity values obtained from: 1) field examples; 2) laboratory tests; and, 3) theoretical models.

.1.2 Field examples

.1.2.1 Materials and methods

A total of 7 ERT profiles (A, B, C, D, E, F and G) have been performed in different gypsum formations along the Ebro and Vallès-Penedès Basins and in the South Pyrenean Foredeep (NE Spain; figure 4.1). The measurements of the apparent electrical resistivity have been made with a SYSCAL PRO switch with 48 electrodes separated by 10, 5, 2, 1 or 0.5 meters

between them (depending on the investigation depth), using internal power supply. Although many different arrays are used in electrical prospecting (Ma et al. 1997; Furman et al. 2003; Szalai and Szarka 2008), the selected arrays in our research were Wenner-Schlumberger and Dipole-Dipole, using the most suitable (depending the presence of structures with horizontal or lateral variations, respectively) in each case. The program used to carry out the inversion of the acquired data is RES2DINV, which uses the smoothness-constrained least-squares method (deGroot-Hedlin and Constable 1990; Sasaki 1992; Loke and Baker 1996) in its inversion routine.

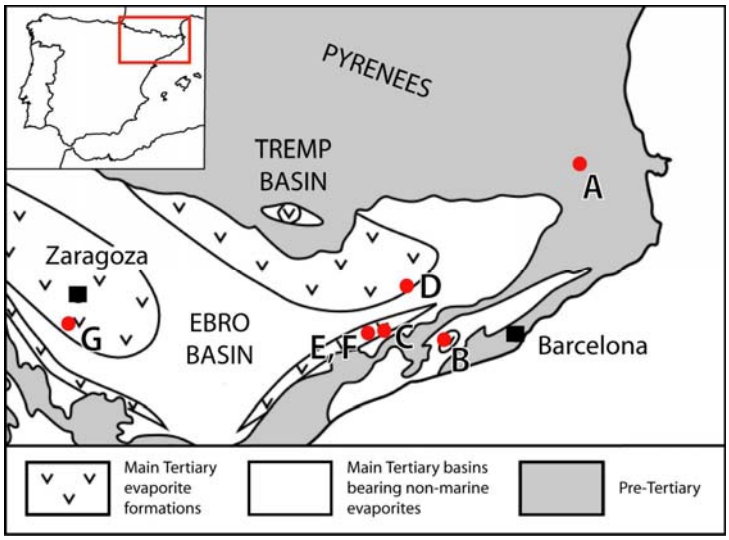

Figure 4.1: Distribution of evaporite formations in the Tertiary basins of central and northern Spain indicating the location of the seven studied ERT profiles (A to G; modified from Ortí et al. 2010).

According to the solubility of gypsum of 2.4 g/l (at normal conditions), the amount of non-gypsum minerals was quantified by dissolving 0.5 g of powdered gypsum samples (collected from the studied formations) in 250 ml of distilled water; the solutions were shaken for 24 hours and subsequently filtered. The remnant after filtering corresponds to the non-soluble impurities of the gypsum rock (lutites, carbonates, quartz, etc.), which has been quantified.

.1.2.2 Results and discussion

The ERT sections acquired in the Ebro and Vallès-Penedès Basins and in the South Pyrenean Foredeep are presented below (from higher to lower gypsum purity):

(A) South Pyrenean Foredeep: A thick evaporitic marine deposit took place during the Lutetian (Middle Eocene) in the eastern Pyrenees (Rosell and Pueyo 1997). Anhydrite (and halite) rocks have been described at depth in boreholes (Carrillo 2009), while secondary gypsum (coming from the hydration of anhydrite) is found in outcrops; the evaporite body is mainly constituted of graynish banded to massive microcrystalline gypsum. Close to the village of Sant Joan les Fonts (Girona province), gypsum rocks outcrop between clay levels (figure 4.2A), attributed to the Beuda Gypsum Unit (Carrillo 2009). The measured purity of a gypsum sample is 98% gypsum. An ERT profile has been carried out near the outcrop in order to evaluate the electrical response of the gypsum-pure layer. The inverted ERT line (figure 4.3A) shows a 5 m thick resistive body, with a mean value of electrical resistivity around 10^3 ohm.m, which clearly corresponds to the purest evaporite layer (layer A in figure 4.4A).

(B) Vallès-Penedès Basin: During the evolution of the Vallès-Penedès Basin, several transgressive pulses in the Burdigalian (Early Miocene) led to partial flooding of the western part of the basin and promoting the precipitation of the Vilobí Gypsum Unit (Ortí and Pueyo 1976; Bitzer 2004). At the western part of the Vilobí del Penedès village (Barcelona province), extensive extraction took place in the last century. The deposit is mainly constituted of banded gypsum alternating with thin lutite-carbonate laminae (figure 4.2B); scarce nodular-entherolithic lithofacies are also recognized. Outcropping gypsum is micro- to macrocrystalline (up to several centimeters in length) secondary (coming from the hydration of anhydrite). The mean gypsum mineral content from the exploited rocks had a purity of 85-87% (personal communication from the chemistry technician of the exploitation body, 2009), while our analyzed gypsum sample displayed a slightly higher purity (92%); but this sample is not representative of the whole deposit, which is less pure. The ERT profile (figure 4.3B) permits us to interpret the presence of an overlying clay level, offering a low electrical resistivity values (around 10 ohm.m), and a shallow body with intermediate resistivity corresponding to a calcarenite layer (which outcrops close to the studied area). The top of the gypsum body is identified at 13 m depth (level B in figure 4.4B), showing higher resistivity values (between 700 and 10^3 ohm.m). There is a low resistive structure between the two main gypsum bodies (figure 4.3B).

(C) Catalan margin of the Ebro Basin: The SE of the Catalan margin of the Ebro Basin recorded during the Eocene-Oligocene several evaporitic lacustrine events (Ortí et al. 2007). Nearby the village of Pira (Tarragona, Spain) in the Conca de Barberà sector of the Ebro Basin, a gypsum deposit has been studied. The gypsum-rock body has been suitably described by

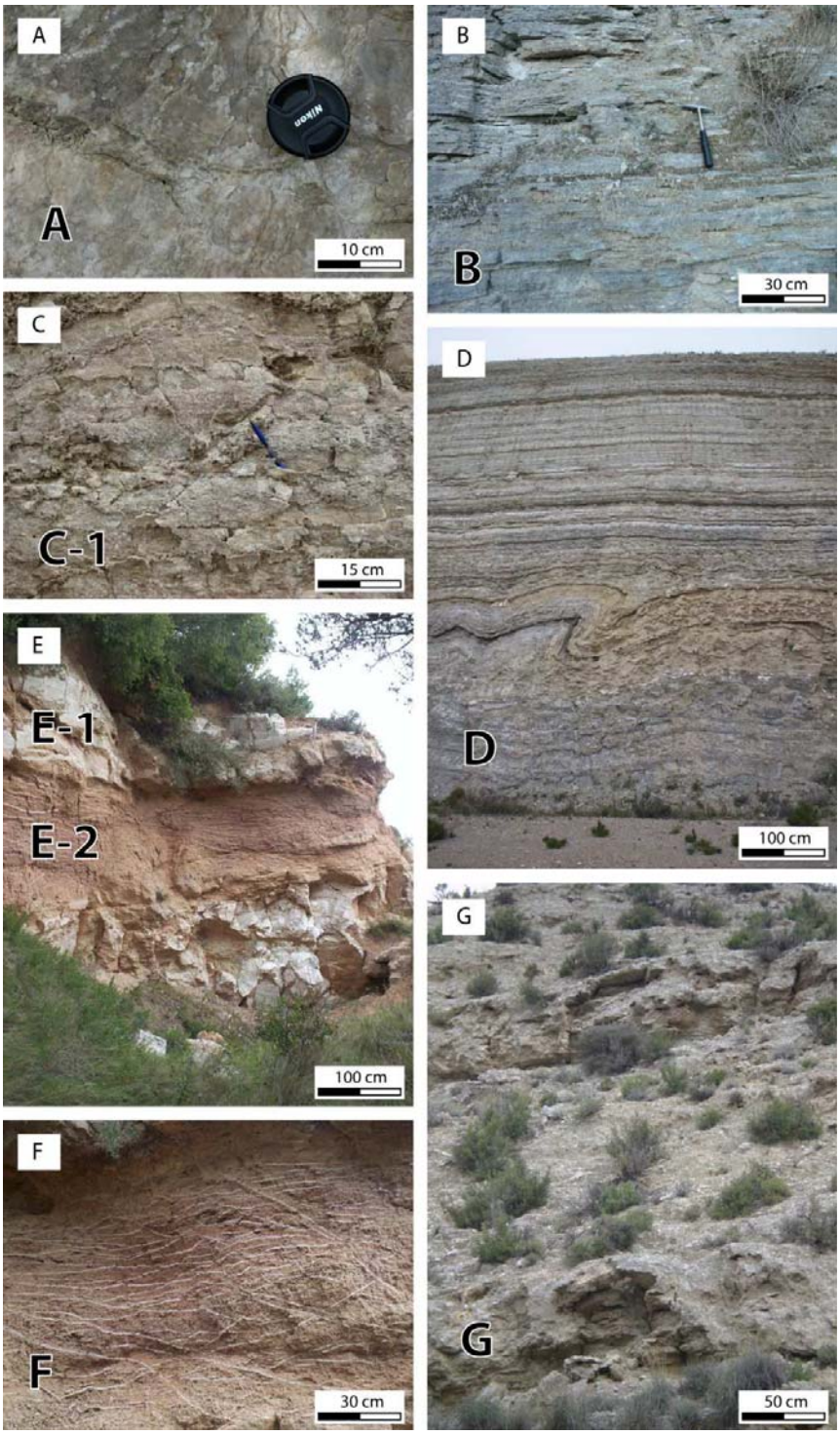

Figure 4.2: Photographs of the different studied areas displaying the different purities of the gypsum rocks in which the ERT profiles were performed. A) Pure gypsum outcrop (A) in Sant Joan Les Fonts village (Girona). B) Laminated pure gypsum (B) in Vilobí del Penedès village (Barcelona). C) Uppermost part of the gypsum deposit (C-1) of Pira village (Tarragona) showing the purest layers. D) Alternation of different intermediate-high purity layers (D) of gypsum in Cervera village (Lleida). E) Intermediate-high gypsum layer (E-1) and lutite layer with satin spar gypsum veins within (E-2) in La Guàrdia de Prats village (Tarragona). F) Lutite layer with gypsum veins within (F) in La Guàrdia de Prats village. G) Impure gypsum deposit (G) in the Montes de Torrero area (Zaragoza). The labels represent the layers described in figures 4.3 and 4.4; the situation of the outcrops is shown in figure 4.1.

means of a borehole, which has been sampled. The measured gypsum-purity from the selected core samples were: 92-94% for the purest levels, 56% for the impurest levels and some from 65 to 72 % in the thin-gypsum embedded in a lutite body. Gypsum layers in this outcrop are constituted of microcrystalline reddish to greenish secondary gypsum, massive to diffusely banded-laminated; nodules of pure white microcrystalline (alabastrine) gypsum are enclosed in the gypsum mass (figure 4.2C), which were extensively exploited as sculpture alabaster for ornamental purposes and gypsum for construction since the fourteenth century and up to the 1970s. The ERT image (figure 4.3C) shows a layer (0.9 m depth) with an electrical resistivity value of 1000 ohm.m, corresponding to the C-1 layer (figure 4.4C); the resistivity decreases rapidly, reaching 50 ohm.m in the underlying sediments (C-3 layer, figure 4.4C). This value is probably slightly higher than the real value because it is displayed at the bottom of the profile, where the method has the lowest sensitivity. The transition between the impure gypsum layer and the bottom values are bounded to the gypsum bearing lutites (C-2 layer, figure 4.4C). The study of this deposit is further explained in the chapter 6 of this thesis.

(D) Catalan margin of the Ebro Basin: The Talavera Gypsum Unit was registered in the Catalan margin of the Ebro Basin during a pulse of lacustrine evaporitic precipitation (lowermost Oligocene; Ortí et al. 2007); several gypsum levels are intercalated in alternation with grey lutites and marls. The study has been carried out near to the village of Briançó (Cervera area, Lleida province). During the construction of the highway some nearby hills exposed the sedimentary deposit; the ERT profile was performed on the top of a hill. The evaporite sequence is made of laminated-banded and nodular secondary gypsum layers (few centimeters to 2 m thick) alternating with lutite rich levels (under 1 m thick, figure 4.2D). The two collected and analyzed samples indicate that gypsum content varies between 68% and 75%, thus, the mean purity of the deposit is around 70% in gypsum content. The electrical imaging displays a quite homogeneous body with an electrical resistivity value between 150 and 500 ohm.m, in accordance with the outcropping unit (figure 4.3D, layer D in figure 4.4D). The homogeneity is due to the sensitivity of the method, which is not capable of distinguishing the different levels. A low resistive anomaly is placed in the right part of the ERT line, which can be interpreted as lateral changes in the sedimentary structures. The increasing of the resistivity values in the bottom of the profile probably reveals the presence of a purer gypsum body (not outcropping in the studied wall).

(E) Catalan margin of the Ebro Basin: The La Guàrdia Gypsum Unit is located stratigraphycally below the Pira Gypsum Unit (Ortí et al. 2007), introduced above, and thus belonging to the same geological setting. The upper part of this unit crops out to the north of

the La Guàrdia de Prats village (Tarragona province), where it consists of reddish gypsum layers, less than 4 m thick in general, which have been the subject of small exploitations, alternating with metric to decametric lutite (and conglomerate) bodies. The lutite layers occasionally are cut by horizontal to about 45º dipping satin spar gypsum veins (cements of fibrous gypsum in veins); visually estimated gypsum content of these lutite levels is around 10%. The sequence has four levels which are from bottom to top (figure 4.2E): A) High purity microcrystalline to nodular secondary gypsum body; B) Lutite layer with gypsum veins of 2 m thick, corresponds to E-2 layer (figure 4.4E); C) Massive to nodular microcrystalline secondary gypsum layer with a measured purity of 73% and 1 to 2 m thick, corresponds to E-1 layer (figure 4.4E); D) 2-3 m of quaternary reddish deposit. An ERT profile has been carried out in this area (figure 4.3E), which displays a set of values ranging from 200 to 500 ohm.m for the E-1 gypsum layer (72% of gypsum content). The structure of the E-2 layer with gypsum veins is not well defined in the profile; the measures have been affected by the most resistive layers above and below (which increases the real resistivity value), but in any case this body displays a range of values from 30 to 100 ohm.m, the expected value is around 10 ohm.m for this level with veins.

(F) Catalan margin of the Ebro Basin: The profile F (figure 4.3F) has been performed 500 meters far from the profile E, thus also prospecting La Guàrdia Gypsum Unit (Ortí et al. 2007). The profile has been carried out directly over a 2 m-thick lutite layer cut by satin spar gypsum (figure 4.2F), overlying a gypsum body. The electrical imaging (figure 4.3F) shows a body with 10 ohm.m of electrical resistivity value which is interpreted to correspond to the gypsum-rich lutite level (layer F in figure 4.4F). Below this body the resistivity value increases until 1000 ohm.m, corresponding to the higher gypsum-purity body.

(G) Ebro Basin: During the construction of the Spanish high velocity train (AVE) railways, some boreholes crossing the Zaragoza Gypsum and Anhydrite Formation were performed in the area of the Montes de Torrero (Zaragoza province). This Miocene formation, hundreds of m thick, was deposited in the Aragón sector of the Ebro basin; it is mainly constituted of anhydrite, glauberite and halite at depth (also thenardite in small quantities), while gypsum is the main evaporite mineral in exposed areas sulphates; the presence of marl and clay is ubiquitous (Ortí 2000; Salvany 2009). Impure secondary gypsum rocks coming from anhydrite or glauberite hydration were cut by the boreholes. The 35 m of the B4 borehole cut an impure gypsum body, similar to the outcropping materials (figure 4.2G), with an estimated

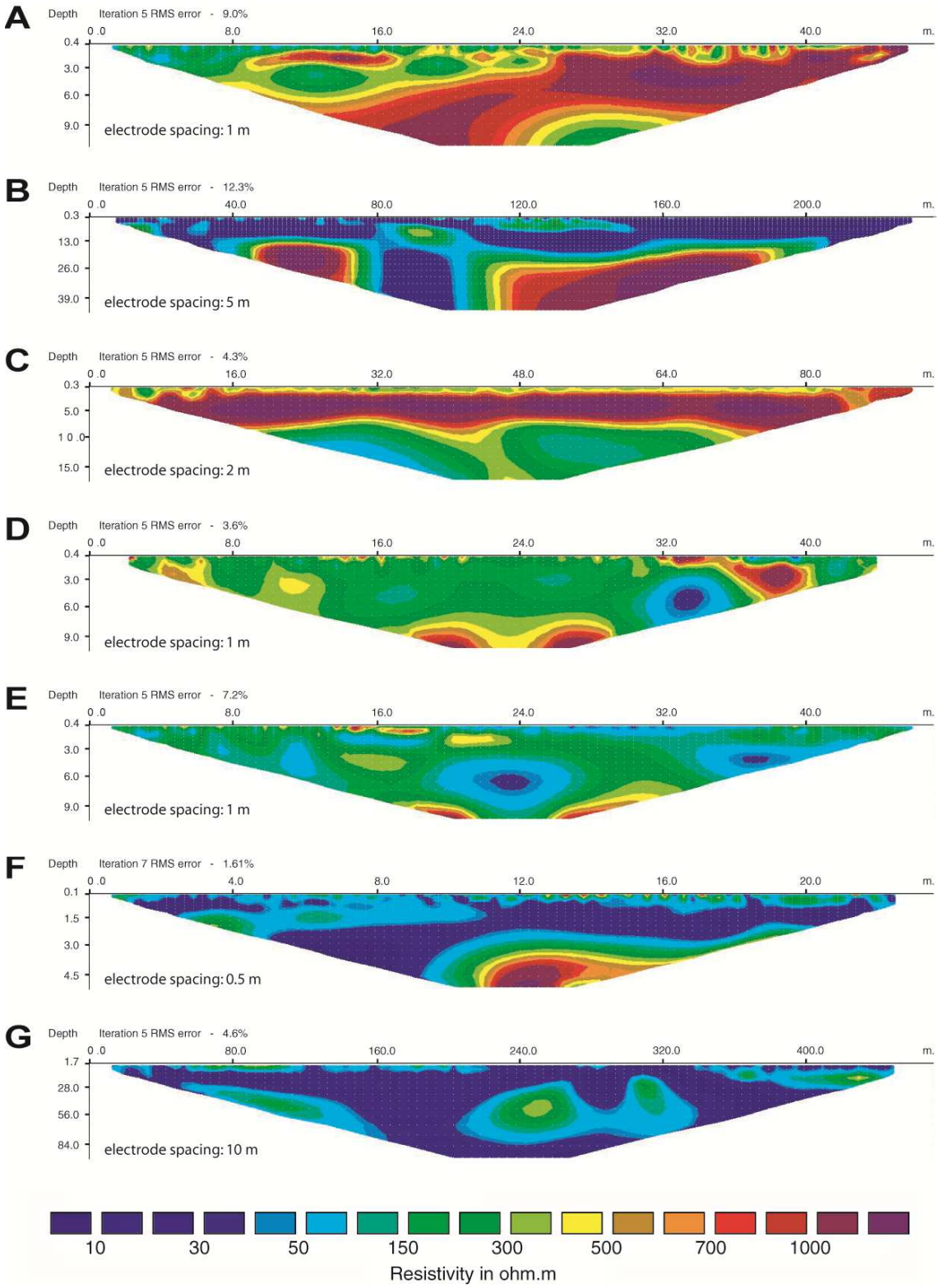

Figure 4.3: Inverted data of the electrical resistivity tomography lines for the different areas studied (A to G, same location and profiles than in figures 4.1 and 4.2).

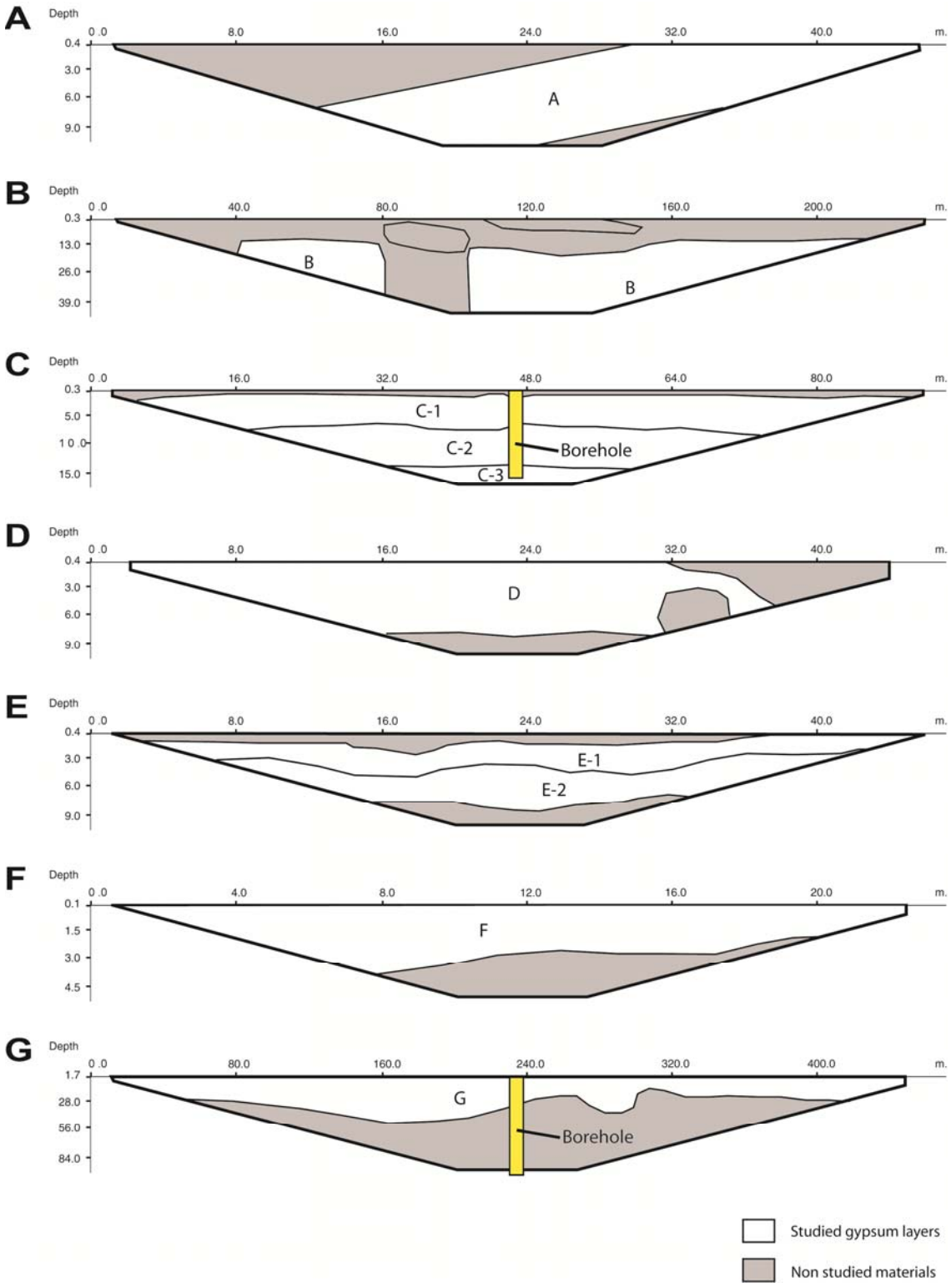

Figure 4.4: Lithological interpretation of the ERT profiles (A to G, same location and profiles as in figures 4.1, 4.2 and 4.3). The sulphate layers are displayed with white color.

gypsum content of 20-40%. The ERT profile (figure 4.3G) shows low electrical resistivity values for this gypsum impure layer (10-20 ohm.m; layer G in figure 4.4G). The secondary gypsum-glauberite contact is at 35 m depth in the B4 borehole; nevertheless, the abundant presence of lutite in the glauberite deposit (also accompanied by anhydrite at depth) masks the resistivity response of such anhydrous evaporites and tends to decrease the values, thus being similar to those of the impure gypsum rocks.

.1.3 Laboratory essays

.1.3.1 Materials and methods

Some laboratory tests have been previously carried out by many authors in order to measure the electrical response of several geologic materials (Daily et al. 1995; Ewanic et al. 2001; Giao et al. 2003; Vanhala et al. 2009; Rusell and Barker 2010; among others). These authors mainly focused on the study of clays (and lutites) because of their relative low electrical resistivity values. The conductivity properties of different mineral crystals was also studied under laboratory conditions by Telkes (1950), Bleaney and Bleaney (1976), Orellana (1972) and Halpern (1998) among others, giving a wide range of resistivity values.

However, the study of the electrical resistivity response of whole rocks or aggregates with medium-high resistivity is poorly developed. The electrical behavior of bulk rocks or isolated mineral crystals is substantially different given that electrical current tends to spread along the contacts between the crystals and/or along the lowest resistive minerals (clays). In our research, the composition of different gypsum rocks with changing purities has been simulated in order to quantify the changes in the measured resistivity values.

Nevertheless, because the laboratory conditions differ from those of the field (humidity, measuring scale, heterogeneities, etc.), it is to be expected that the resistivity values obtained would be slightly different than those obtained in field conditions. This is principally because, at field scale, the electrical current can find some conductive paths to spread due to the anisotropy of the terrain while at a smaller scale the samples are more homogeneous, thus they could display a more resistive behavior.

Several tests have been performed in laboratory conditions in order to measure the electrical resistivity response of gypsum rocks. Eleven sample-pills have been made with a

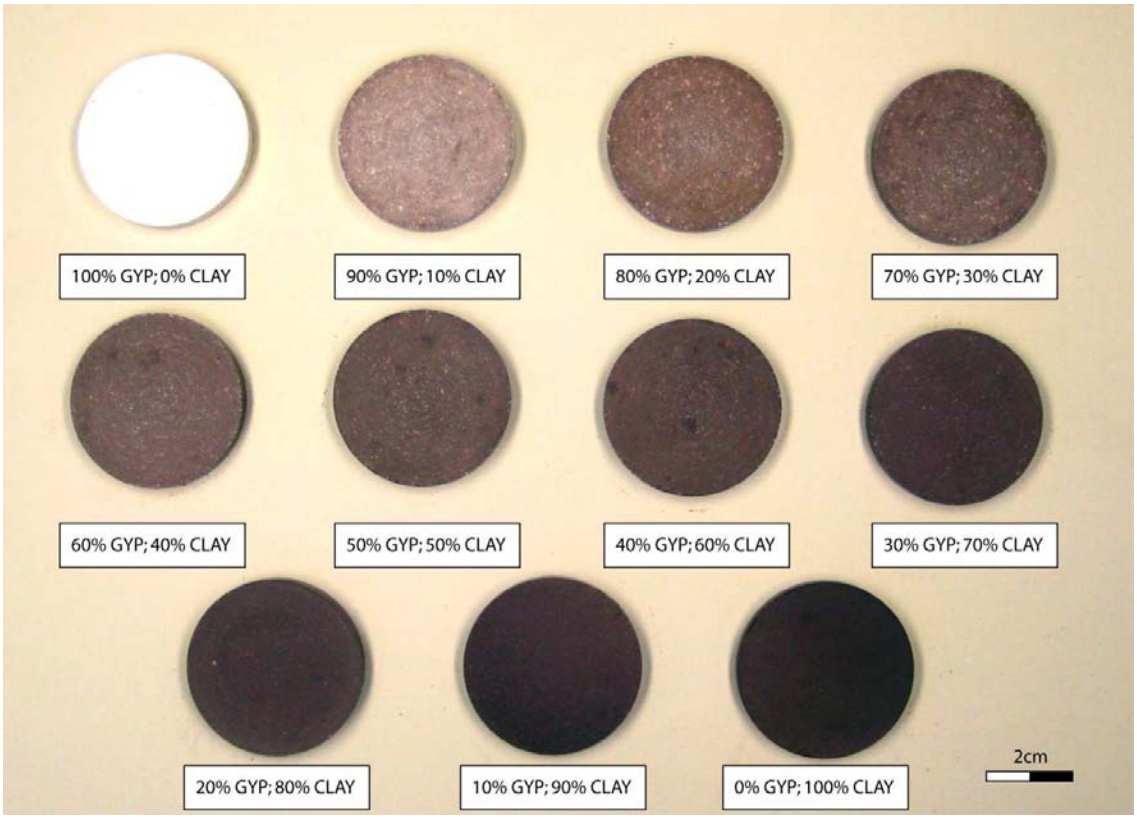

Figure 4.5: Sample pills made using mixtures of powdered clays and CaSO4·2H2O laboratory reagent in different proportions (100% to 0% gypsum contents in intervals of 10%).

mixture of different proportions of powdered clay and gypsum, simulating real geological samples, and an electrical current has been applied through them. The pills are made of mixed red clays (collected in the field) with pure dihydrated calcium sulphate (Panreac PA-ACS $CaSO_4 \cdot 2H_2O$ laboratory reagent ref. 131235.1210, simulating natural gypsum). The clays were dried in a furnace at 40ºC for 2 days and powdered. The bulk and clay mineral composition of the clay fraction was studied by X-ray diffraction as randomly oriented powder and oriented preparations (air-dried, glycolated and heated at 550ºC) in a Siemens D-500 diffractometer. The clay-gypsum mixture varies from 0 to 100% of gypsum (intervals of 10%; figure 4.5). Each pill was prepared under overpressure conditions (press machine at 200kN) for 60 seconds. In order to support the cementation of the pills, the blended powder-samples were slightly wetted with sprayed distilled water before the pressing process; otherwise the pills are brittle. Additionally, the sample was hand-pressed with a whirling movement before connecting the press in order to distribute the sample homogeneously. After this process, the pills were left to dry for 48 hours. The resulting pills, 13.5 g in weight, took a cylindrical shape, 2 cm in radius. The thicknesses of the cylinders, measured with a vernier caliper, were around 0.5cm.

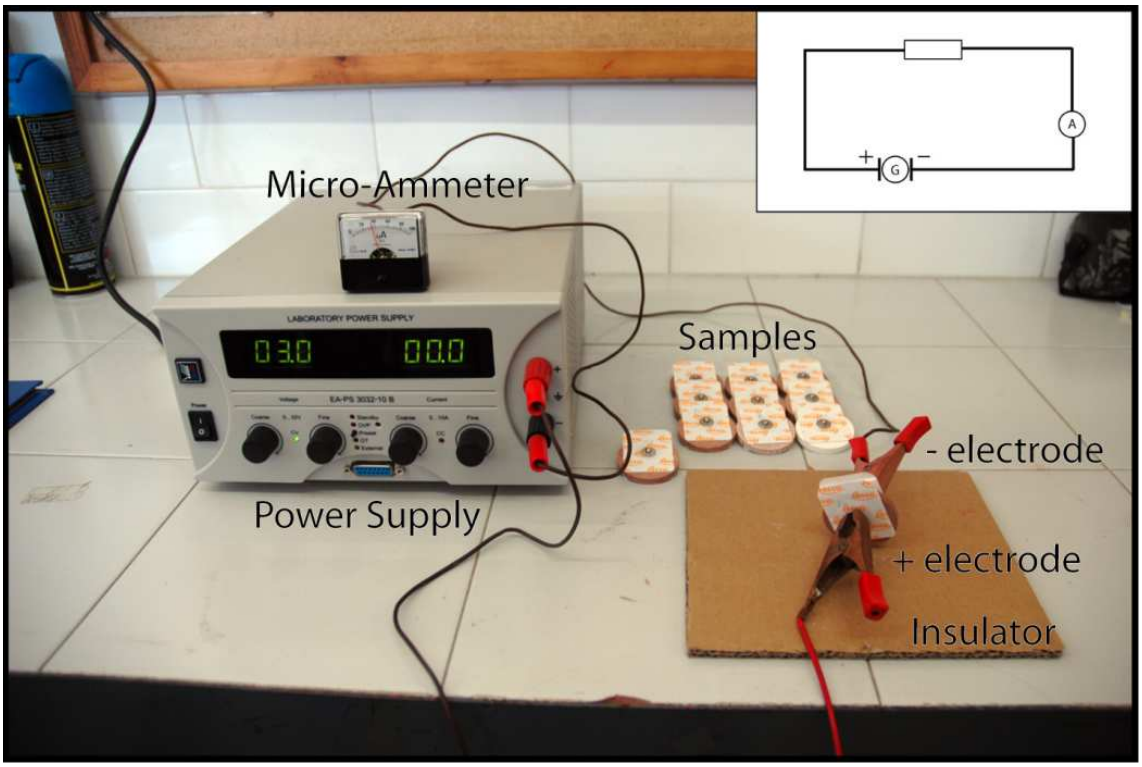

Figure 4.6: Electrical circuit developed to measure the electrical resistivity values of the pill samples; it consists of a switchable laboratory power-supply, two electrodes and a micro-ammeter.

An electrical circuit was developed under laboratory conditions in order to perform the measurements of the electrical resistivity of the pills (figure 4.6). The power source was a laboratory DC converter power supply (0 to 32 V); the negative-pole wire incorporated a micro-ammeter (0-100 microamps) or a nano-ammeter (with a range of ±200 nA and 0.1 nA resolution and an accuracy of 2%) for the pills with highest resistivity (the ones ranging from 70 to 100% in gypsum purity). The electrodes used on the samples are made of stickers with metallic buttons, in accordance with the UNE 21-303-33 regulation (1983). The button has a conductive gel in the sticking side, forming a 0.75 cm-radius circled face (which will be considered the surface of the electrode). The gel is directly connected to the samples. These sticker-electrodes are connected to both sides of the samples in the same position (because the electrical current runs perpendicularly to the samples). The buttons of the electrodes are clamped by the pins of the wires which connect both poles of the circuit, with the sample acting as a resistance. The sample is laid upon an insulator made of paperboard to avoid electrical leakages. Ohm's law can be applied to calculate the conductivity (σ) or resistivity (ρ) of the sample for a known current density (j) and field (E) (equation 1):

Equation 4.1: $$j = \sigma E = E / \rho$$

It is possible to measure the resistance (*R*) of the samples. As the thickness (*L*) of the sample and the surface area of the electrode (*S*) are known, the electrical resistivity (ρ) can be calculated in another form of the Ohm's law (equation 2):

Equation 4.2: $$R = \rho L / S$$

Some different essays were carried out before the adequate development of the definitive electrical circuit. The selected electrodes and the design of the circuit are in accordance with the UNE 21-303-33 regulation, which states that the measures have to be done with a DC and stable current. Previous tests were performed within a wide range of voltage between 1 and 200 V, taking into account that higher voltages could induce superficial secondary electrical currents and that the presence of any type of low resistivity impurities in the rock (as lutites) could overcharge the sample and generate small fractures.

As it was observed that no leakages occurred within the range of 1-200 V, a guard-ring around the electrodes is not required. The readings were made with a voltage of 3 V for the essays in which the micro-ammeter was used and 0.1 or 0.2 V in the ones in which the nano-ammeter was used. An amperage above 1 A in the power supply has been shown to be enough; the use of different amperage conditions higher than 1 A does not display different measures, thus an amperage of 2 A has been selected for the experiences. The sample measurements have been carried out at 10, 30, 60, 180 and 300 seconds.

.1.3.2 Results and discussion

During the laboratory measurement the amperage conditions of the power supply remained constant (2 A) and the measured amperage in the gypsum-clay pills varied from below (<1 μA) to above (>100 μA) the detection limits of the micro-ammeter. As noted before, in the case in which the readings in the micro-ammeter were below its detection limit (for the case of pills with purities from 70 to 100%) the nano-ammeter was connected. The results indicate that the micro-ammeter is most suitable for optimum measures in lutite-rich pills (up to 70 % in gypsum content, table 4.2).

The sample measures in the laboratory circuit have been carried out at 10, 30, 60, 180 and 300 seconds. Measurements clearly tend to decrease at higher intervals of time and the fall is more sudden when increasing lutite contents (lower gypsum purity), due to the polarization of the enclosed clay minerals (table 4.2, figure 4.7). The injected current is

% Gypsum	Thickness (cm)	Voltage (V)	10s (µA)	30s (µA)	60s (µA)	180s (µA)	300s (µA)	Resistivity (ohm.m)	Transect
0%	0,460	3	100	95	90	84	78	11	1
10%	0,505	3	70	69	66	61	56	15	1
20%	0,470	3	65	64	64	62	59	17	1
30%	0,480	3	53	52	52	49	46	20	1
40%	0,490	3	45	44	43	40	38	24	1
50%	0,490	3	29	29	28	27	26	37	1
60%	0,500	3	9	9	9	9	9	117	2
70%	0,500	0.1	0,160	0,155	0,157	0,164	0,161	221	3
80%	0,510	0.1	0,130	0,122	0,124	0,121	0,119	267	3
90%	0,510	0.1	0,090	0,090	0,094	0,100	0,960	385	3
100%	0,505	0.2	0,082	0,079	0,086	0,089	0.079	853	3

Table 4.2: Results of the laboratory measurements, depending on the time of measurement, the applied voltage and the thickness of the samples. The electrical resistivity value is calculated from the measurements performed at 10 seconds. Transect (1, 2, 3) corresponds to the areas defined in figure 4.8.

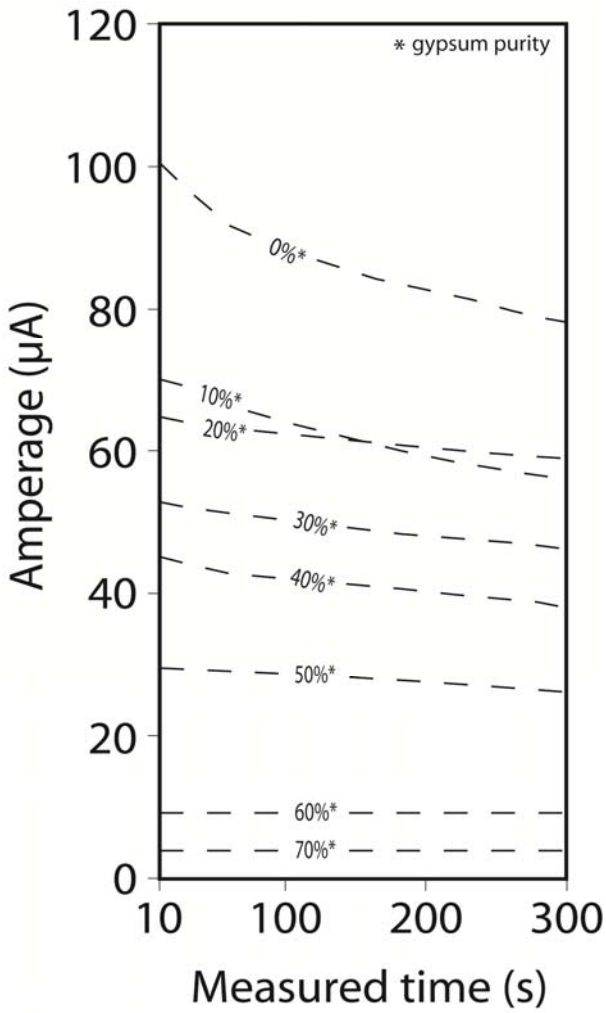

Figure 4.7: Plot showing the relationship between the measured amperage and the time of measurement for different gypsum contents in the samples. 10s, 30s, 60s and 180s are the measured time.

continuous and the material would not polarize supposedly; nevertheless, it is clearly shown that the samples with large clay composition tend to be polarized while increasing the reading time when the electrical current flows. The most polarized sample is the purest clay-pill (100% clay) while polarization stops in a 60 % gypsum, 40 % clay mixture. It is considered that the optimum measuring time is 10 seconds, in order to be representative of the measures of the geoelectrical methods (as they do not inject a continuous electrical current during a long period of time). The variations in the readings in the case of the samples with gypsum purity of 70% or above are not of significance.

The results of the laboratory tests show an increasing electrical resistivity value pattern clearly related to the gypsum-purity in the samples. The results from the measures can be divided into three transects (table 4.2, figure 4.8):

1) The first transect corresponds to the measurements obtained in pills up to approximately 55% in gypsum-purity. The electrical resistivity value slightly increases from about 11 ohm.m (0 % gypsum) to 37 ohm.m (50 % gypsum).

2) The second part is a transitional area between 1 and 3 (55 to 70 %, both included); the electrical resistivity values of the pills with a thickness of 0.5 cm increase rapidly but still inside the range of the micro-ammeter scale of measures.

3) The third part of the plot corresponds to the 0.5 cm-thick richest-gypsum pills (>70 %); the electrical resistivity values cannot be measured with the micro-ammeter because they are below the detection limit (readings <1 μA), while with the nano-ammeter samples show signals within the ammeter range. The 70, 80, 90 and 100% purity pills show a clear increasing trend in the final calculated resistivity values, with the 100% pill being the most resistive.

The result from the X-ray diffraction of the powdered clay shows that it is composed of chlorite, kaolinite and illite with minor amounts of calcite, quartz, feldspars and gypsum. It has to be noted that, while the powdered clay fraction of the pills can be directly compared with the geological clay or lutite units, the powdered gypsum fraction is texturally and crystallographically different from the gypsum deposits. The $CaSO_4 \cdot 2H_2O$ reagent used is cryptocrystalline (finely crystalline), while common gypsum rocks are from micro- to macrocrystalline (up to several meters in the largest selenite crystals). Thus, these values cannot be considered to be representative of real gypsum rocks.

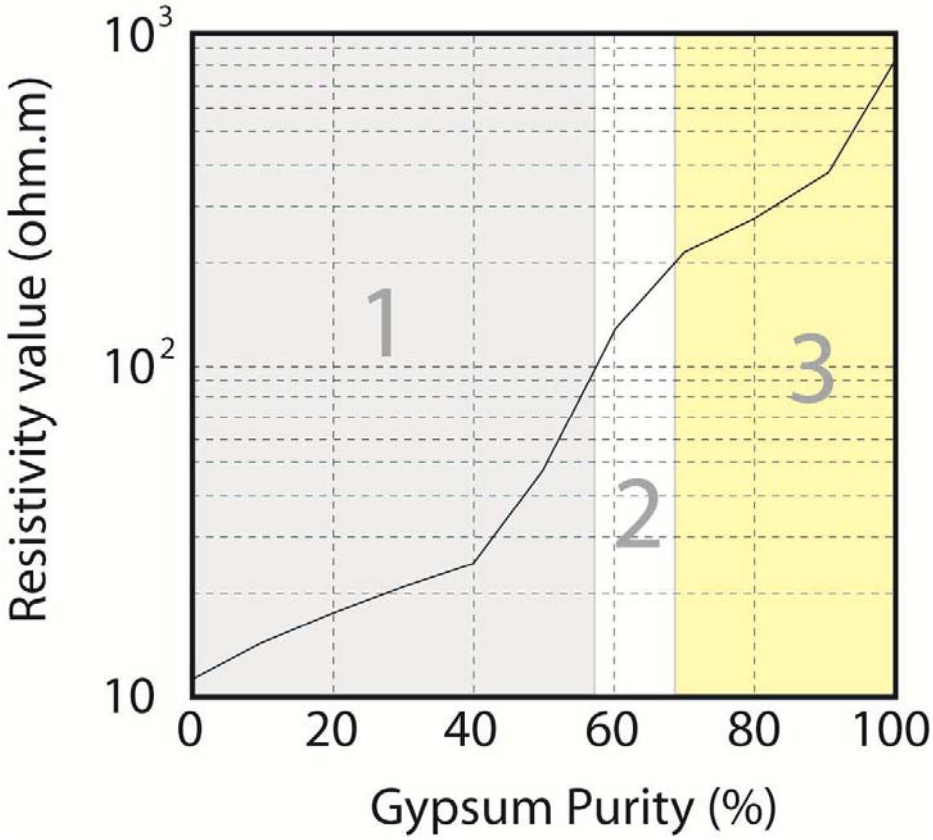

Figure 4.8: Semi-logarithmic plot representing the results of the electrical resistivity laboratory measures in synthetic gypsum pills. 1, 2 and 3 are the observed different trends.

.1.4 Theoretical models

.1.4.1 Materials and methods

On the basis that gypsum rocks are formed essentially by gypsum mineral and enclosed lutites together with accompanying carbonates, quartz, celestite… (figure 4.9), a set of theoretical models has been elaborated, representing homogeneous gypsum deposits (figure 4.10). The RES2DMOD program has been used; this program calculates the electrical apparent resistivity pseudosection for a user-defined 2D underground model (Loke 2002). This program has been widely applied in order to simulate the acquisition of field data in a known medium (Cornacchiulo and Bagtzoglou 2004; Maillet et al. 2005; Srinivasamoorthy et al. 2009). Sumanovac and Dominkovic (2007) used RES2DMOD program to determine the resolution of a block model in a homogeneous mean.

The models of this study are formed of a block of theoretical gypsum rock and a conductive background (with a resistivity of 1 ohm.m in order to facilitate the passage of

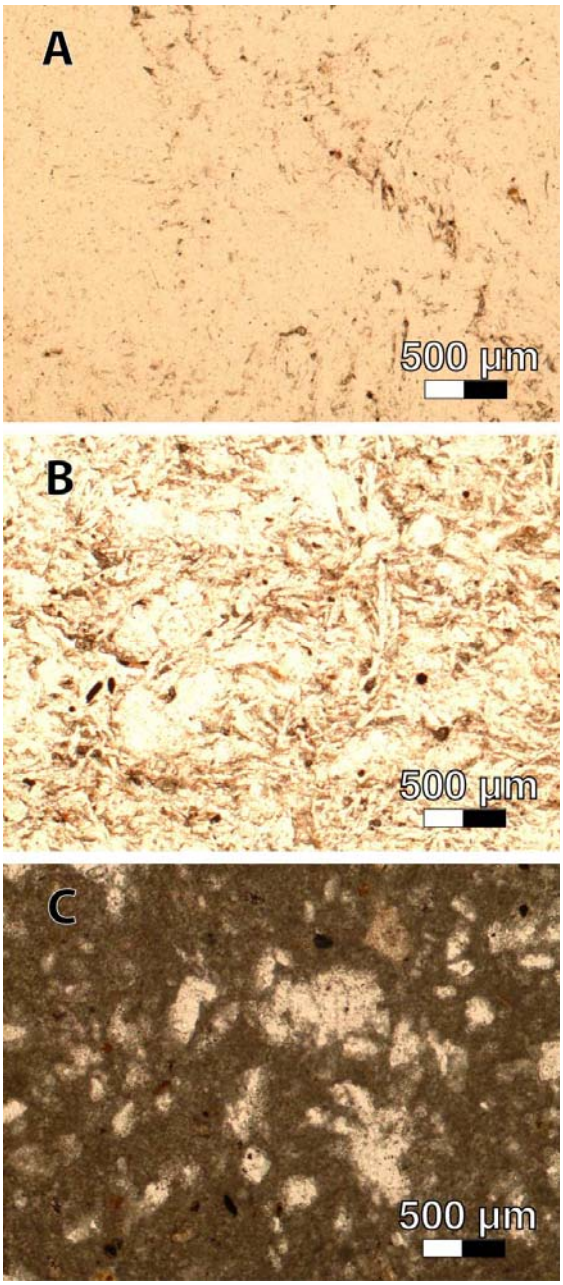

Figure 4.9: Photomicrograph (plane polarized light) of different gypsum rocks showing A) pure gypsum, B) impure gypsum and C) gypsum-rich lutites.

electrical current). The model blocks are composed by 1760 small squares and each square has a value of 10 or 10^3 ohm.m depending on whether it represents lutite or gypsum mineral. The size of the block was selected in order to be large enough to let the inversion achieve the values of the original model. The shape of a block was chosen at the expense of a continuous layer to support the absence of artifacts. The conductive mean which surrounds the model

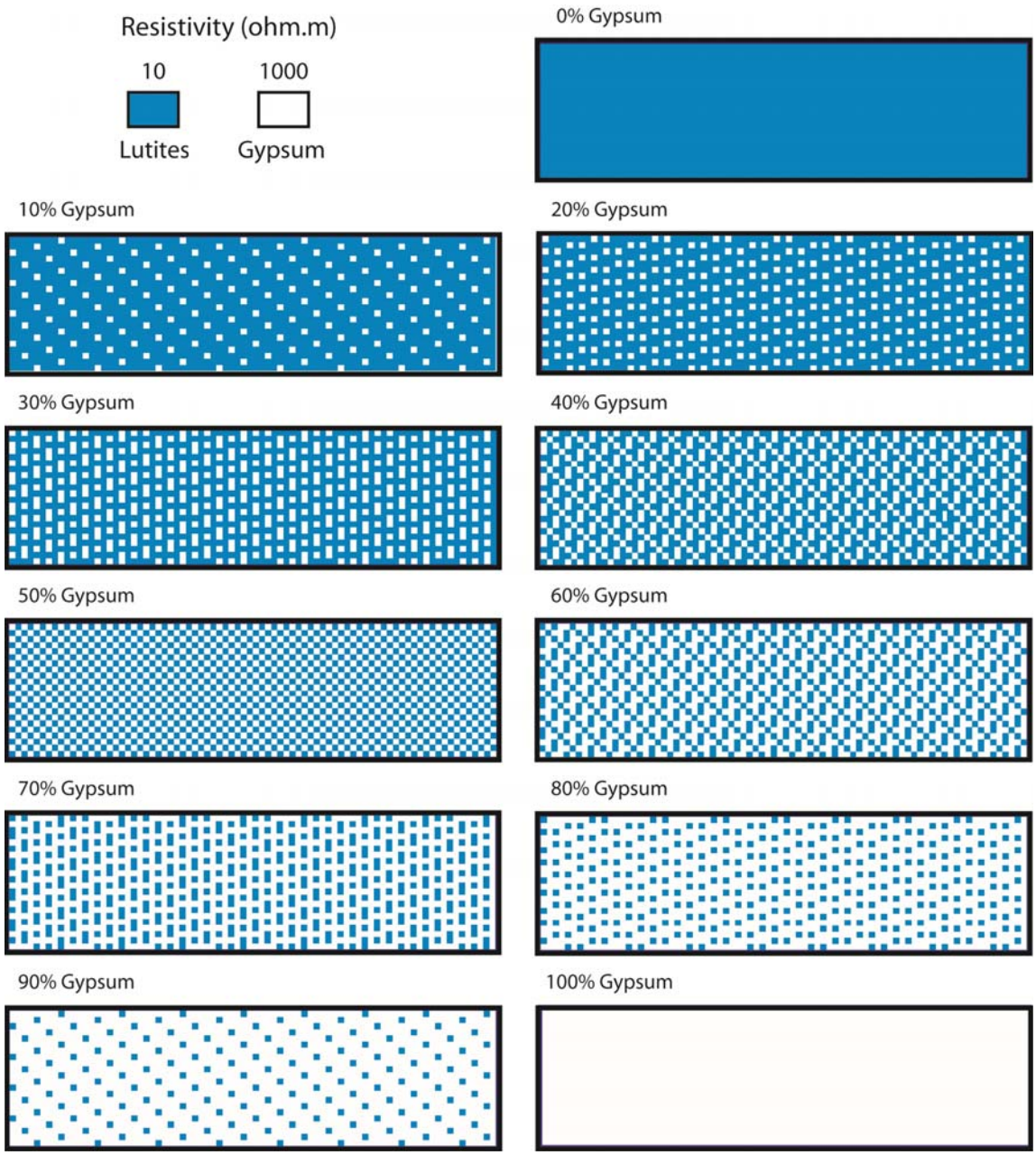

Figure 4.10: Model blocks elaborated with the RES2DMOD program; each block represents a gypsum rock body with changing composition (gypsum versus lutite percentages).

block has the lowest electrical resistivity value possible in order to optimize the sensitivity within the gypsum rock block.

The composition of the block has been changed for every model displaying different purities of the gypsum rock block from 0% to 100% (in gypsum mineral composition). These models represent the morphological distribution of the rock at the micro-scale for different purities. In the models, the scattered phase (meaning lutites) has been represented as small

and homogeneously dispersed impurities within the model block. The sensitivity of the method is unable to distinguish these impurities; thus, the inversion of the data does represent the theoretical gypsum body as a homogeneous deposit. The inversion has been carried out with the program RES2DINV as in the case of the field data.

Lutites are accompanying materials in gypsum lithofacies commonly; they are disseminated in the rock (solid inclusions within the gypsum crystals or in the intercrystalline porosity) or as separate lutite laminae or beds. The purity of gypsum deposits (percentage of gypsum minerals) can vary widely, even in the same evaporite unit. For deposits consisting of alternating laminated-to-banded levels with different purities (gypsum-lutites), the geoelectrical image would be generally interpreted as homogeneous bodies represented by the mean value of the deposit, alternating lithologies would - or would not - be identified after the inversion routine of the data depending on the thickness of the levels due to the sensitivity of the method. A set of theoretical models has been elaborated, representing an evaporitic deposit constituted of gypsum rocks with disseminated enclosing lutites (figure 4.10).

.1.4.2 Results and discussion

Into the initial user-defined model (figure 4.11A), the mean electrical value assigned to gypsum mineral was 1000 ohm.m and 10 ohm.m for lutites (essentially clay and marl), thus the real block-resistivity values for the two extreme cases of gypsum rock content of 0% and 100% is 10 ohm.m and 1000 ohm.m, respectively. In the inversion of data we can iterate the program until it achieves these values at the point of the model block with highest resistivity value (reference point in figure 4.11C). The methodology used with the rest of the models (with purity from 10% to 90%) consists of performing the same number of iterations and checking the resistivity value at the same point of the model block. This value would represent the electrical resistivity value for a gypsum rock with the purity selected on the initial model. Different arrays were tried during the elaboration of the models: Wenner alpha, inline Dipole-Dipole, Pole Dipole and Wenner Schlumberger. These arrays are commonly used in geoelectrical surveys and they have different sensitivity distributions. Wenner-Schlumberger was the most stable between iterations when reaching the expected value in the reference models (100% and 0% of purity).

The electrode spacing selected was 2 meters, in order to have an adequate investigation depth for the models. With this procedure an apparent-resistivity pseudosection of the model was obtained (figure 4.11B). Afterwards, the data from the direct model were

inverted. The inverted value of the resistivity section has been checked at the centre of the model (at a horizontal position of 47 meters and a depth of 9.60 meters) in different iterations (figure 4.11C). Between iterations 17 and 18, the value of resistivity reached 1000 ohm.m at this point (994.45 ohm.m in the 17th iteration and 1022.40 ohm.m in the 18th iteration, respectively). The obtained value is considered to be correct as we know that the original model block had a resistivity of 1000 ohm.m.

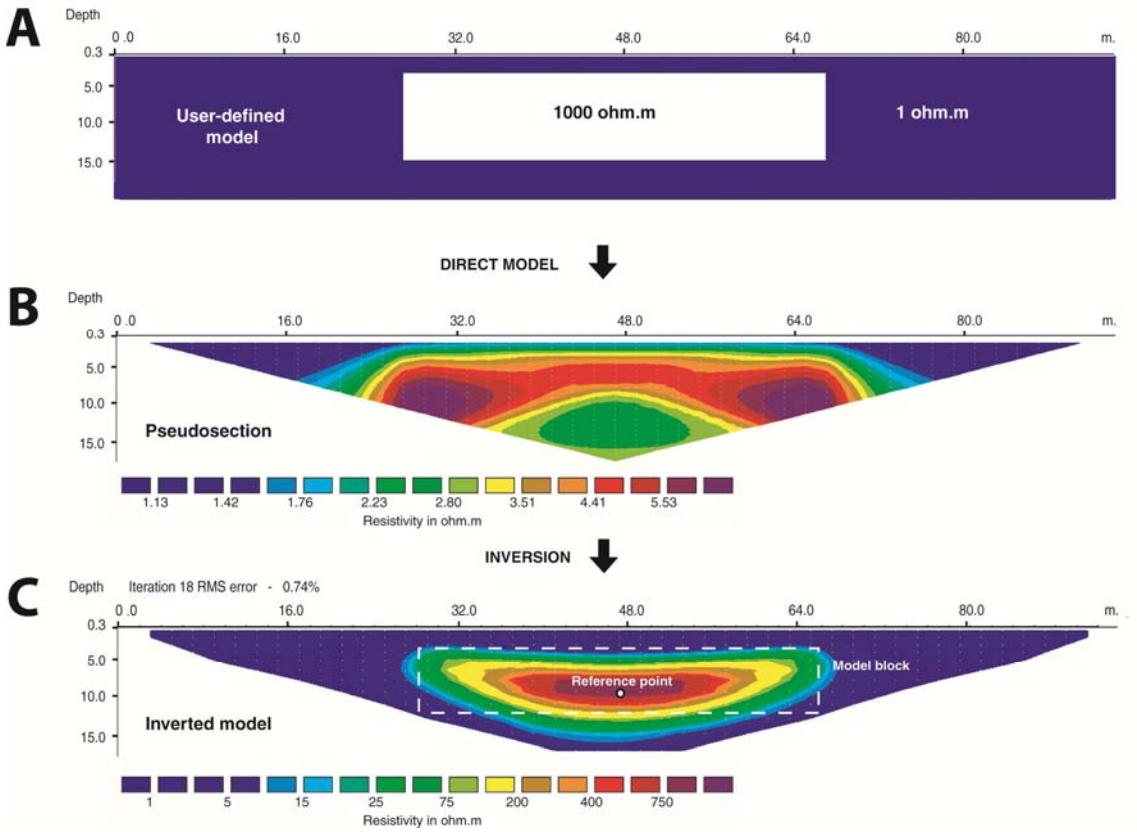

Figure 4.11: Sketch of the theoretical calculation process, showing a model-block representing a 100% pure gypsum rock (A). From the theoretical model an apparent resistivity value pseudosection is calculated (B) and afterwards the data are inverted by performing 17-18 iterations. The value of the calculated resistivity is checked at a reference point (C), which must have the same value as that of the initial model. The process is repeated with different model blocks with initially unknown bulk electrical resistivity values.

In the case of the model with 0% purity, it displays a value of 12.15 ohm.m and 12.16 ohm.m in iterations 17 and 18, respectively, which is also close to initially considered electrical resistivity value in the original model (10 ohm.m; figure 4.12).

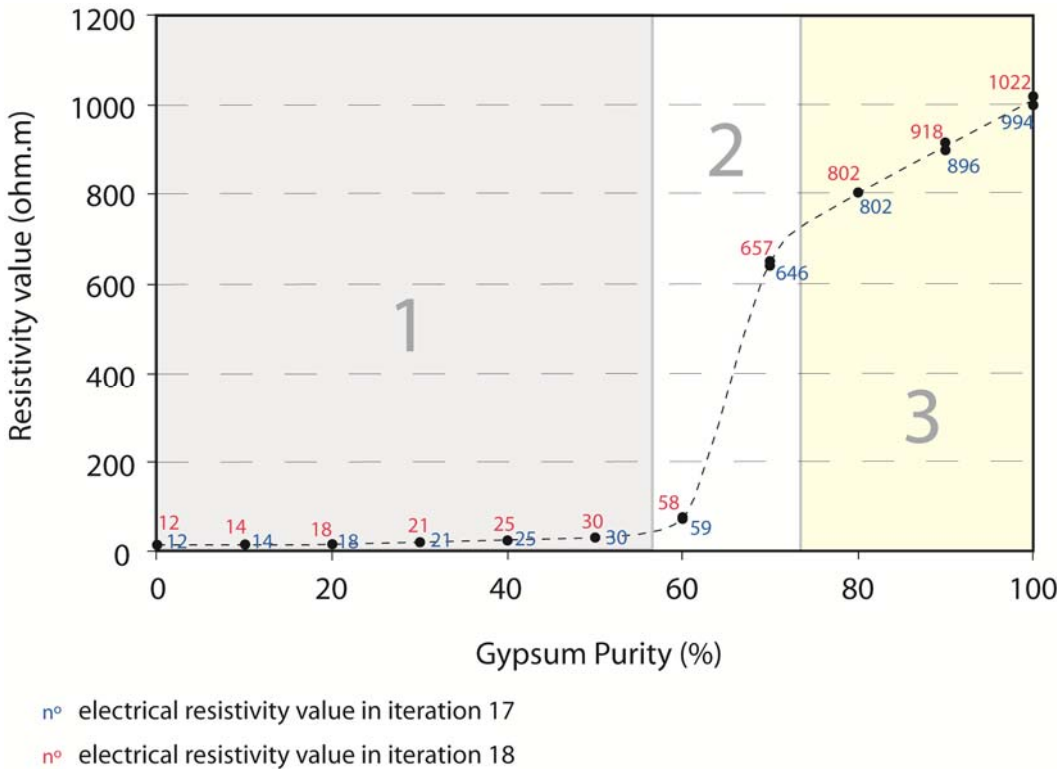

Figure 4.12: Electrical resistivity values calculated from the theoretical models from gypsum bodies, with purity ranging from 0 to 100%. The values show the difference in the calculation between the iterations 17 and 18. The three different transects of resistivity are displayed in the background with different colours.

The inverted resistivity values obtained for the reference point X=47.00 m, Z=-9.60 m in iterations 17 and 18 for the different purity models have been collected in order to relate them with the gypsum contents of the rocks. The trends in the plot of calculated resistivity from iterations 17 and 18 are almost coincident, and only slightly diverge in the 90% and 100% purity values (figure 4.12). Because of this, the mean trend between both lines can be considered. The results show three different transects:

1) Purity of the rock from 0% to 55%; the plot shows a slightly increasing trend in the electrical resistivity values while increasing the purity.

2) Between 55 and 75% of gypsum purity; the value of resistivity increases exponentially.

3) Above to 75% of gypsum contents; the slope of the curve tends to diminish until the maximum resistivity value for pure gypsum rocks. The absolute resistivity values obtained and the gypsum-purity vs. resistivity pattern are very similar to those obtained after laboratory essays (figure 4.8).

.1.5 Geoelectrical classification of gypsum rocks:

Theoretical, laboratory and field data have been obtained; they show three differentiated trends (figure 4.13):

1) The first trend of resistivity values are from 0 to approximately 55% gypsum purity (obtained from interpolation; part 1 in figure 4.13). The electrical resistivity value increases from 10 (in the impurest member) to approximately 50 ohm.m (55% of gypsum content), in accordance with the expected resistivity for lutites. In the case of the field examples, some rocks bodies placed within this range of purity show electrical resistivity values slightly higher (but below 100 ohm.m). This is due to the position of these layers below a resistive material and/or located at depth (bottom of the ERT profile), where the sensitivity of the method is lower and then the values obtained are less reliable (layers C-3 and E-2 in the profiles C and E, respectively).

2) The second trend ranges from 55 to 75% (obtained from interpolation, these values are approximate) in gypsum purity and is characterized by an important resistivity values variation with little composition change (part 2 in figure 4.13), where the electrical resistivity increases exponentially, and ranging from 100 to 700 ohm.m.

3) The third trend ranges from 75 to 100% in gypsum purity (part 3 in figure 4.13). The electrical resistivity value increases continuously with the increasing of the purity and offers a range of values of 700-1000 ohm.m (from the impurest to the purest, respectively). In the case of the laboratory pill measurements, the values obtained are substantially higher than those obtained in both theoretical calculations and field measures, which is due to the crypto- to microcrystalline nature of the pills, in contrast to the micro- to macrocrystalline textures of the gypsum rocks. This type of gypsum is considered as economically profitable when displaying values of electrical resistivity above 800 ohm.m (80% in purity).

The existence of these three differentiated trends would be bound to the connection between lutite particles within the gypsum rock. In the case of the impurest members, the electrical current avoids the gypsum crystals, and preferentially flows along the lutite matrix (due to its conductive nature; figure 4.14A). The resistivity value slightly increases with increasing gypsum content in lutite bodies; nevertheless, the influence of these disseminated gypsum particles is scarce, and the lutite presence is the main controlling factor in their geoelectrical response. When the gypsum-purity achieves the minimum value to obtain a gypsum supported rock (corresponding to the packing coefficient of a simple cubic packing -

52%-; figure 4.14B) the electrical current is forced to pass through the gypsum crystals, even with a partially connected lutite matrix.

This represents the boundary between transects 1 and 2. Increasing the purity of the rock, would achieve the packing coefficient of compact cubic package (74%), which would correspond to a gypsum crystals supported texture (78 % intercrystalline porosity in a 2D representation; figure 4.14C). In this package, the lutite particles are no connected but scattered; thus the electrical resistivity measurements are dominated by the presence of the gypsum crystals. Figure 4.14C represents the transition between transects 2 to 3 in figure 4.13. In the purest gypsum rocks (>75 % approximately; part 3 of figure 4.13) the resistivity increase tends to become stable; the electrical current is forced to flow through the gypsum crystals (figure 14D).

A general classification of gypsum rocks on the basis of their geoelectrical response and purity has been defined (table 4.3); three types of gypsum rocks are distinguished

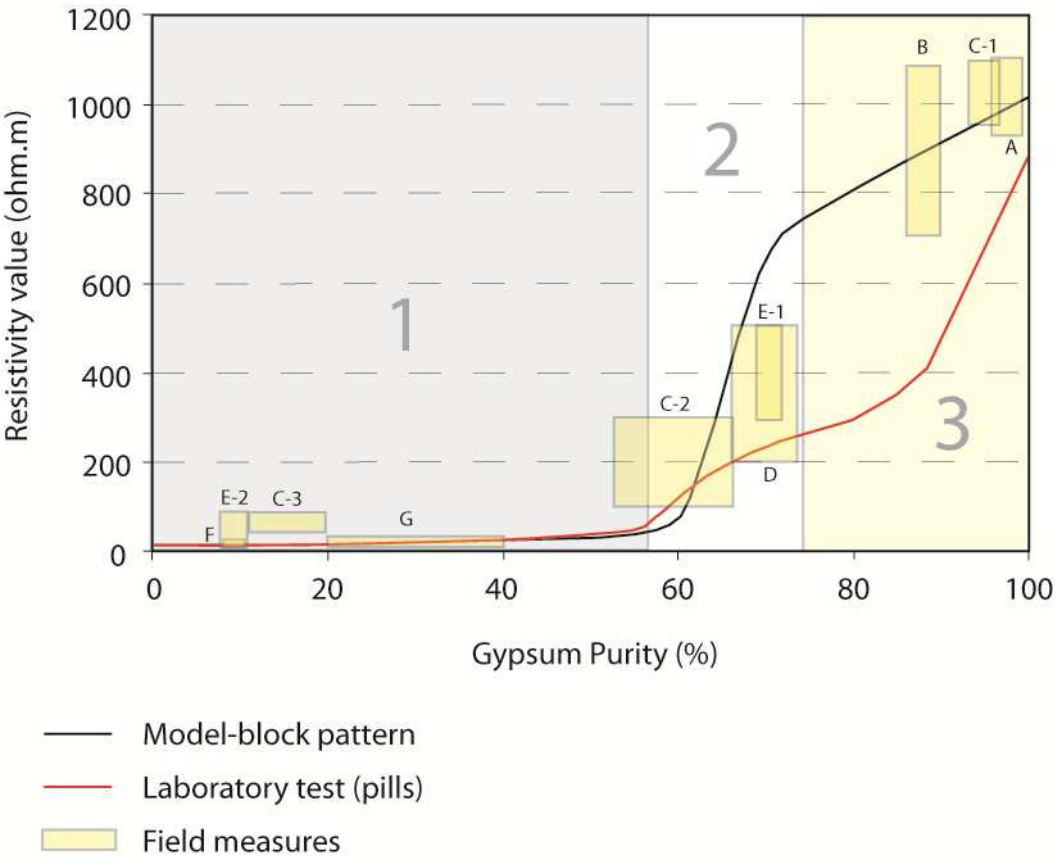

Figure 4.13: Integrated plot combining the results of theoretical calculations, laboratory tests and the ranges of purity and electrical resistivity values measured in the field examples.

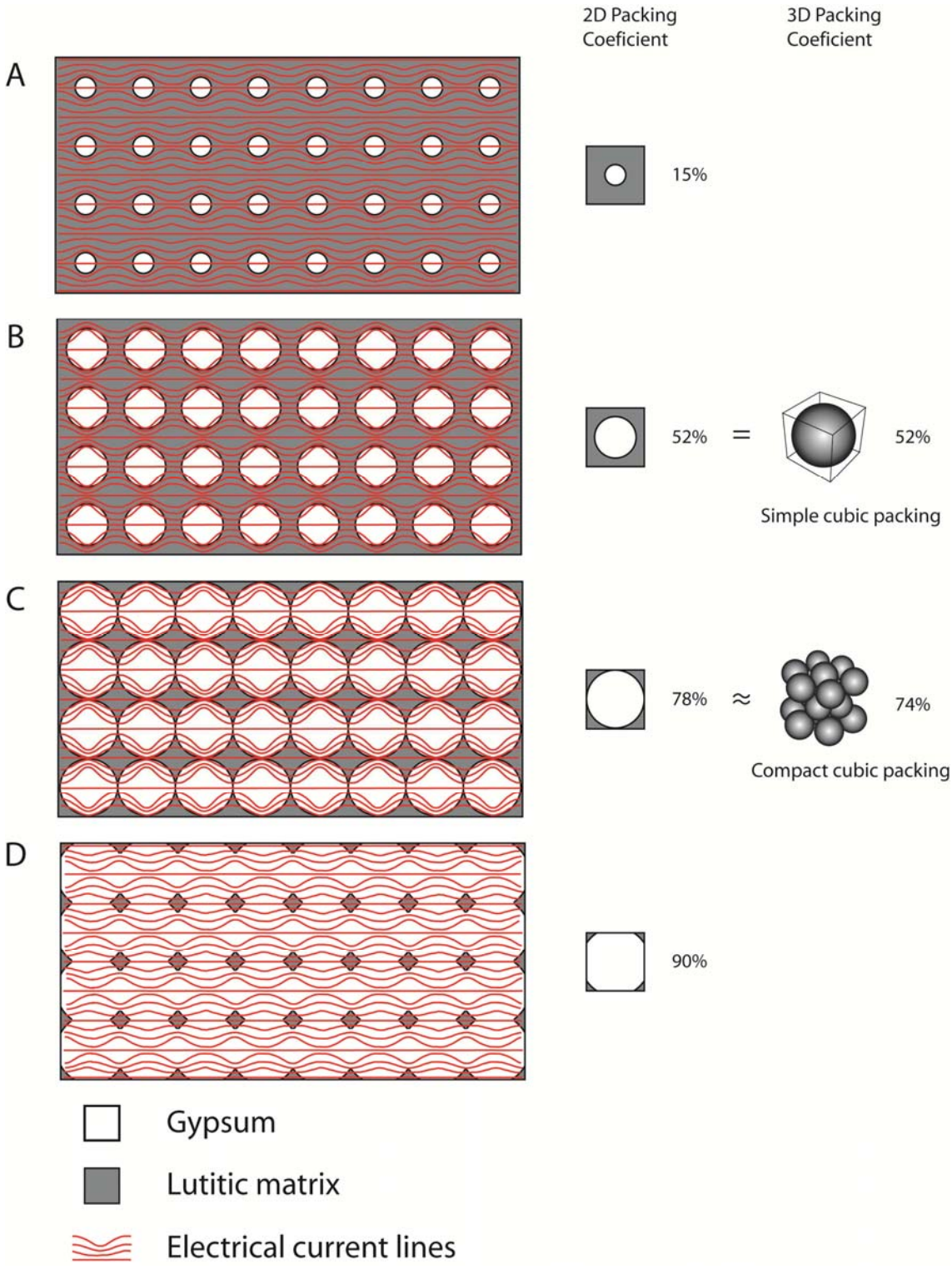

Figure 4.14: Two-dimensional simplified representation of the electrical current circulation through different gypsum rocks. A to D sketches represent different gypsum contents in the rocks, from 15 to 90 %, respectively.

corresponding to the three different trends shown in the figure 4.13: 1) Pure gypsum, displaying an electrical resistivity response from 700 to 1000 ohm.m and >75% in gypsum

mineral. 2) Transitional (dirty) gypsum; belonging to the transition zone with about 75 to 55% in gypsum mineral composition and a range of electrical resistivity value from 100 to 700 ohm.m. 3) Lutites and rich-gypsum lutites; having a large amount of lutites on their composition (higher than 45%), and showing an electrical resistivity range of values between 10 and 100 ohm.m. This trend is based in the general tendencies observed in field, theoretical calculations and laboratory measurements (disregarding the pills with gypsum purity above of 70% because they have been considered not to be representative). This trend could be taken as a reference in future surveys in this type of rocks. The results are limited by the sensitivity of the method used, as in other surveys.

Type of Gypsum rock	Gypsum purity (%)	Resistivity value (ohm.m)
Pure Gypsum	75 - 100	700 - 1000
Transitional Gypsum (Dirty gypsum)	55 - 75	100 - 700
Lutites and gypsum-rich lutites	0 - 55	10 - 100

Table 4.3: Geoelectrical classification of gypsum rocks, depending on their gypsum purities.

.1.6 Percolation theory and Hashin-Shtrikman bounds in gypsum rocks

Physical properties of rocks are mainly functions of their microstructure and of their chemical-mineralogical composition. Two dominant mathematical formalisms – effective medium theory (EMT) and percolation theory – can be used to answer this problem. The EMT (Kirkpatrick 1973) approximation is quite good for rocks with quasi-uniform distributions where only a small degree of heterogeneity is observed, although they cannot describe correctly the phenomenon of clustering (Guéguen et al. 1997) when the heterogeneity is large. Moreover, the knowledge of the geometric distribution and connectivity of the minor phase is of great importance.

Percolation theory describes the medium in terms of probabilities of the connectivity but does not provide bulk physical properties. Here, we propose a method to determine the physical properties of composite materials that combines the EMT and the percolation theory. On one hand, the EMT is used to calculate the bounds of the physical properties depending on the amount of the matrix phase present. These limits correspond to the two extreme situations where the matrix phase is totally interconnected or disconnected. On the other hand, the percolation theory is used to determine the probability of having a connected or interconnected matrix phase assuming that it is distributed in a single cube distribution.

The percolation theory states that in a cluster with a component randomly distributed (meaning the lutitic matrix for this case) there is a percolation threshold which represent the minimal quantity of the component to display a long-range connectivity (Stauffer and Aharony 1985). This theory has been widely used to predict characteristics of rocks as the connection of their porosity or fractures (Glover et al. 2000; Karmakar et al. 2003; Wang et al. 2007). When the component quantity is below the percolation threshold, the cluster is no more percolant.

In our system the percolation is bounded to the spreading of electrical current along the matrix which is much more conductive than the gypsum phase. Gypsum component is dielectric (act as resistance) and it is avoided by the electrical current while the system is percolant. But when percolation threshold is surpassed, the electrical current finds no paths to spread in the matrix and it runs by the gypsum crystals which became into conductive phases. Because of this when the presence of matrix is above 40%, the rock is much conductive without a significant variation in function of the gypsum quantity.

Hashin and Shtrikman (1963) defined the electrical resistivity value bounds (HS bounds) of a bulk rock only from the information of the fractions of each component. These bonds represent the maximum (upper bound) and minimum (lower bound) electrical resistivity value that a rock formed of two different phases with a certain proportion of them can display. With the knowledge of the fraction (γ) and the electrical resistivity value (ρ) of each component it is possible to calculate these upper (HS^+, equation 3) and lower bounds (HS^-, equation 4):

Equation 4.3: $$\rho_{HS^+{}_{1,2}} = \rho_1 \left[1 - \frac{3(1-\gamma_1)(\rho_1-\rho_2)}{3\rho_1-\gamma_1(\rho_1-\rho_2)}\right]$$

Equation 4.4: $$\rho_{HS^-{}_{1,2}} = \rho_2 \left[1 + \frac{3\gamma_1(\rho_1-\rho_2)}{3\rho_2+(1-\gamma_1)(\rho_1-\rho_2)}\right]$$

HS bounds have been calculated for the case of gypsum rocks with different proportions of gypsum and matrix. The electrical resistivity values selected for gypsum and lutite phases have been 1000 and 10 respectively as it has been selected before. These bounds have been compared with the general resistivity trend of the gypsum rocks shown in figure 4.13 and the results show that they match with the lower bound when the gypsum quantity is 60% or less and with the upper bound when the gypsum purity of 70% and above (figure 4.15).

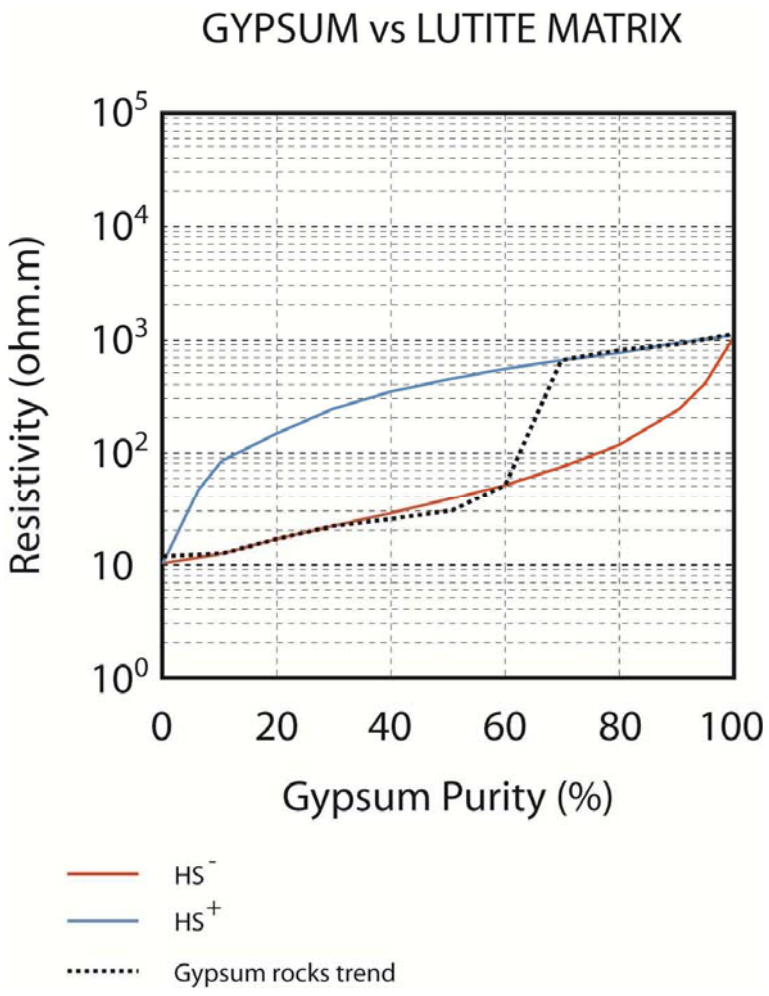

Figure 4.15: Hashin-Shtrikman bounds for gypsum rocks and the trend showed by the field data, laboratory essays and theoretical calculations.

The values obtained between 60 and 70% in gypsum purity would be transitional meaning the percolation threshold. Theoretically the percolation threshold is punctual but in

the case of real rocks transitional values are displayed in this range of composition because the distribution of the components is not totally homogenous.

.2 ANHYDRITE

.2.1 Introduction

Anhydrite is calcium sulphate ($CaSO_4$) and usually has secondary origin but also can be precipitated in sabkha environments in primary processes. Gypsum rocks are extensively affected by diagenetic processes which can change their texture into microcrystalline. They tend to transform into anhydrite when buried because of dehydration and the opposite process also takes place when anhydrite is affected by weathering and superficial waters.

One of the most important problems found while quarrying gypsum is the presence of anhydrite. Comparing with gypsum, anhydrite has different physical properties as higher hardness and density. The drilling machines can be damaged because of this hardness and when an anhydrite body appears, the exploitation must be stopped immediately. Anhydrite is also used in industry for different purposes, but because of the exploitation difficulties it is mainly obtained from dehydration of previously extracted gypsum. Anhydrite (coming from gypsum dehydration) is commonly found at deeply buried units (>500 m, in general), it rarely outcrops because it tends to hydrate and transform into gypsum.

REFERENCE	RESISTIVITY (ohm.m)	AUTHOR'S COMMENTS
Lugo et al. (2008)	1000-11500	The bodies displaying the lowest values are related to the presence of gypsum from the hydration of anhydrite while the highest ones are related to pure anhydrite.
Asfahani and Mohammad (2002)	94-1200	The values are measured by vertical electrical soundings in a gypsum and anhydrite formation.
Choteau et al. (1997)	1000	Anhydrite appears in an halite-karnalite-tachyhydrite secuence.
Robinson and Çoruh (1988)	10^9-10^{10}	Anhydrite appears in a summary of different mineral resistivity values
Rider (1986)	10^4-10^{10}	Obtained from diagraphy logs of different sources.
Parkhomenko (1967)	1.0 -10^9	Listed in a summary of different mineral and rock resistivities
Jakosky (1950)	1.0 -10^3 / 1.0-10^5	Low and High resistivity ranges obtained from laboratory measures

Table 4.4: Published electrical resistivity values for anhydrite rocks.

Published electrical resistivity show a large range of values from <100 to 10^{10} ohm.m (table 4.4). The variation in the electrical resistivity value of anhydrite is related to the presence of gypsum in these publications, but the influence of the lutitic matrix is not mentioned. The characterization of the electrical resistivity of anhydrite rocks in the presence of gypsum minerals and lutitic matrix is studied from three different angles, namely numerical modeling, laboratory measurements and field data. Obtained information would help to interpret geoelectrical data in the future surveys on sulphate rocks and to interpret electrical resistivity value of other rock groups formed of various components with different electrical properties.

.2.2 Field Data

.2.2.1 Materials and methods

A total of nine ERT profiles have been performed upon anhydrite rock deposit areas in the South Pyrenean Foredeep and Ebro Basin (North East of Spain; figure 4.16). The examples are presented below starting with the ones performed in quarries (figure 4.16, A to G) and afterwards in areas with no-outcropping evaporites (figure 4.16, H and I). All the profiles performed in quarries show high purity of sulphates and therefore relatively high electrical resistivity values.

A Syscal Pro Switch with 48 electrodes and external power supply has been used to carry out the data acquisition. The electrode spacing for the measures in quarries has been 1, 1.5 or 2 meter depending on the logistical availability. In the profiles performed in no-outcropping evaporites zones the electrode spacing selected has been 10m to increase the investigation depth because anhydrite deposits tend to be under sedimentary basins (else they transform into gypsum; even this process also can take place at depth).

There are many possible array configurations in geophysical prospection; for measuring anhydrite rocks, Wenner-Schlumberger and Dipole-Dipole have been selected depending of the structure under study (Dipole-Dipole has been used in the case of dominating lateral electrical resistivity changes). The apparent resistivity data of performed ERT profiles has been inverted with RES2DINV program. The code consists in the algorithm of smoothness-constrained least squares (deGroot-Hedlin and Constable 1990; Sasaki 1992; Loke

and Barker 1996). The inversion process has been carried out with 5 iterations for each profile. With this number of iterations the data converges in all cases achieving an acceptable RMS error; additional iterations do not vary significantly the RMS error but increase the electrical resistivity value in the low sensitivity areas (this is, the pure sulphate rocks). As it is explained later, the values obtained for inverted electrical resistivity data (with 5 iterations) in expected pure anhydrite bodies are likely to those of apparent ones measured directly on observed anhydrite rocks.

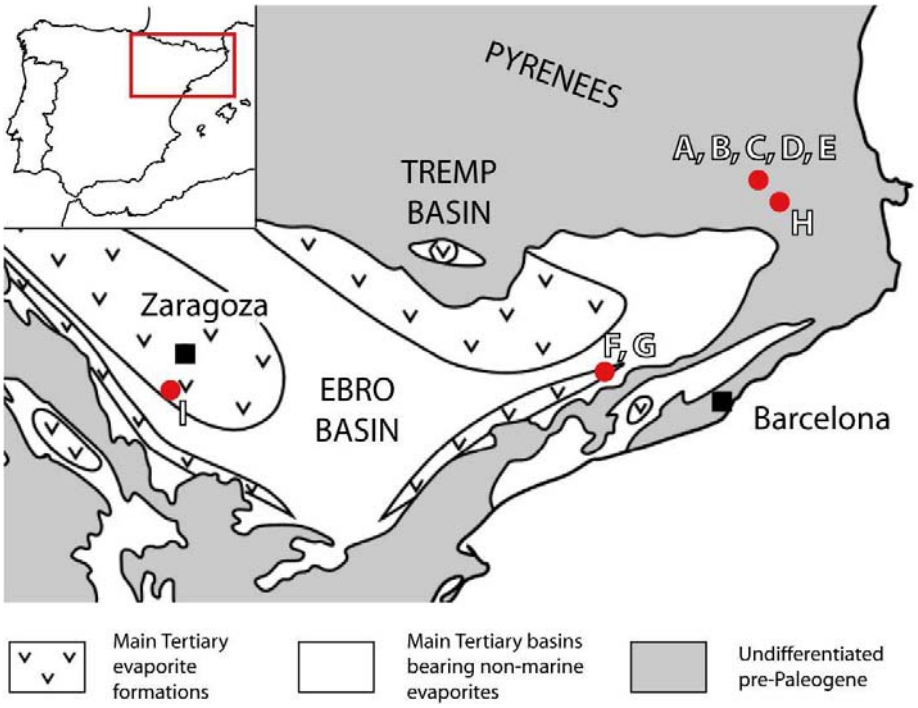

Figure 4.16: Distribution of the evaporite formations in the Tertiary basins northeastern Spain indicating the location of the nine studied ERT profiles (A to I) with red dots (modified from Ortí et al. 2010).

Complementary to the ERT surveys, sulphate samples have been collected in some of the studied areas in order to measure the amount of matrix on them. The samples have been powdered and 0.5g from each one has been dissolved in 250 ml of distilled water in accordance with the solubility in water of calcium sulphate. The solutions have been shaken during 24 hours and filtered afterwards. The residue left after filtering correspond with the non-soluble phases, this is, the lutitic matrix (including carbonates, quartz and other minor

accompaining minerals), which can be weightened and quantified in order to estimate the purity in sulphate phases of the calcium sulphate deposits.

.2.2.2 Geological settings

Beuda area (Girona):

During the Lutetian (Middle Eocene) a large marine evaporitic sequence was deposited in the South Pyrenean Foredeep (Rosell and Pueyo 1997). In La Garrotxa area (eastern Pyrenees) secondary gypsum (as product of the hydration of anhydrite) outcrops extensively and anhydrite has been found in borehole logs with other evaporitic rocks as halite (Carrillo 2009). Close to the village of Beuda (Girona, Spain) there is a quarry in which gypsum is exploited since at least the decade of 1930. There are many gothic sculptures made of alabaster (pure secondary microcrystalline gypsum) in which the geochemical analysis have demonstrated that the raw material was extracted from the Beuda gypsum unit (Inglés et al. 2009).

Nowadays the quarry has been largely developed (figure 4.17A) and anhydrite outcrops in many places in which the exploitation has been stopped because of its presence. The gypsum of Beuda unit came from the hydration of anhydrite and therefore there are still some anhydrite relict bodies embedded in the gypsum. In the walls of the quarry it is possible to observe boundaries between gypsum and anhydrite usually displaying a quite pure anhydrite core and a transition to pure gypsum (figure 4.17B). The purity of the calcium sulphates vary from close to 75% to higher than 90% in certain layers (figure 4.17C). The changes in the purity of both gypsum and anhydrite rocks and the complex geometrical relations between them make these deposits very heterogeneous. In some cases matrix bearing gypsum appears in contact with pure anhydrite (figure 4.17D) and in other cases the anhydrite does not appear as a body but as fragments embedded in gypsum and filled with gypsum veins (figure 4.17E). In other places anhydrite appears massive with little gypsum within (figure 4.17F). Five ERT profiles (figure 4.18, A, B, C, D and E) have been performed in Beuda gypsum quarry. The profile H (figure 4.18H) has been performed in the same formation of the quarry of Beuda, close to the village of Serinyà. In the studied area there are sulphate layers under a cropping field. In the nearby outcrops pure secondary gypsum appears, but in depth, the sulphates would transform into anhydrite as it has been observed in the region (Carrillo 2009).

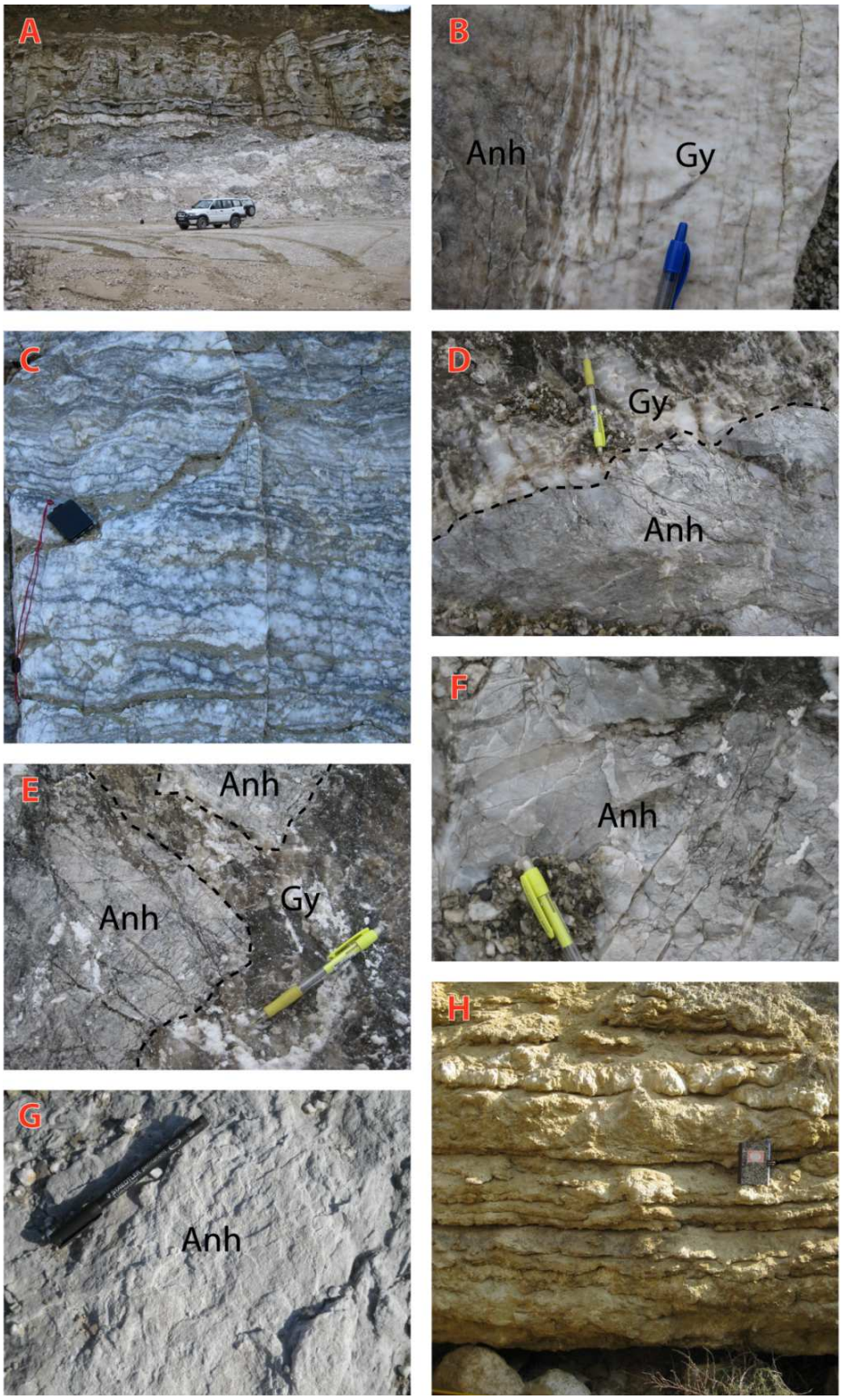

Figure 4.17: Photographs of the areas studied with ERT, A to F are taken in the quarry of Beuda while G is taken in the area of Odena and H in Zaragoza formation. A) general view of the quarry; B) pure gypsum-anhydrite boundary with a interdigitation between them; C) sulphate layers showing less purity than in other areas; D) boundary between pure anhydrite and relatively impure gypsum; E) anhydrite blocks filled with gypsum veins and embedded in a gypsum matrix; F) massive anhydrite with little gypsum within; G) massive anhydrite body; H) impure sulphate layers in Montes de Torrero area.

Odena area (Barcelona):

Marine evaporitic deposition took place during the upper Eocene in the Catalan margin of Ebro basin (Ayora et al. 1994). The Odena gypsum unit was extensively exploited during the XXth century and the region is plenty of abandoned quarries. The profiles F and G have been performed in abandoned quarries near to the village of Odena where anhydrite outcrops (figure 4.17G).

Montes de Torrero area (Zaragoza):

In the Montes de Torrero area (Zaragoza, Spain) there is a Miocene evaporitic formation hundreds of meters thick. During the construction of the Spanish high velocity train (AVE) railways the area was studied by mean of boreholes in which gypsum, anhydrite, glauberite and halite were found among other minerals. This formation has a large quantity of matrix in every layer (Ortí 2000; Salvany 2009). The outcropping materials are mainly gypsum coming from the hydration of anhydrite or glauberite (figure 4.17H) and with more than 50% of matrix (composed of clay and marl). An ERT survey has been performed where the borehole B4 was drilled (figure 4.18I). The log of the borehole shows gypsum until 35 meter depth and below glauberite until 69 meter depth and anhydrite until 80 meter depth with some interbedded layers of halite or glauberite (Salvany 2009). The whole log has important quantity of matrix as it is seen in the surface.

.2.2.3 Results and discussion

In the quarry of Beuda some different areas have been studied. The profiles A, B and C have been performed upon areas in which was found massive anhydrite and afterwards was buried under quarry waste materials. The profiles were spread above the infilling. The result of the inversion for the profiles A and B (figure 4.18, A and B) display an upper part with relatively low electrical resistivity values (between 10 and 200 ohm.m) which would correspond to the quarry waste. Underlying these materials there is a homogeneous body with high resistivity value (up to 10^4 ohm.m) interpreted as pure anhydrite. In the case of profile C, it was performed perpendicularly to profile B.

The inverted resistivity section (figure 4.18C) displays a lateral electrical resistivity variation below the quarry waste layer. With a drilling machine the center part was drilled (no log was recovered) and at arriving 6 meter depth was found high hardness of the rock

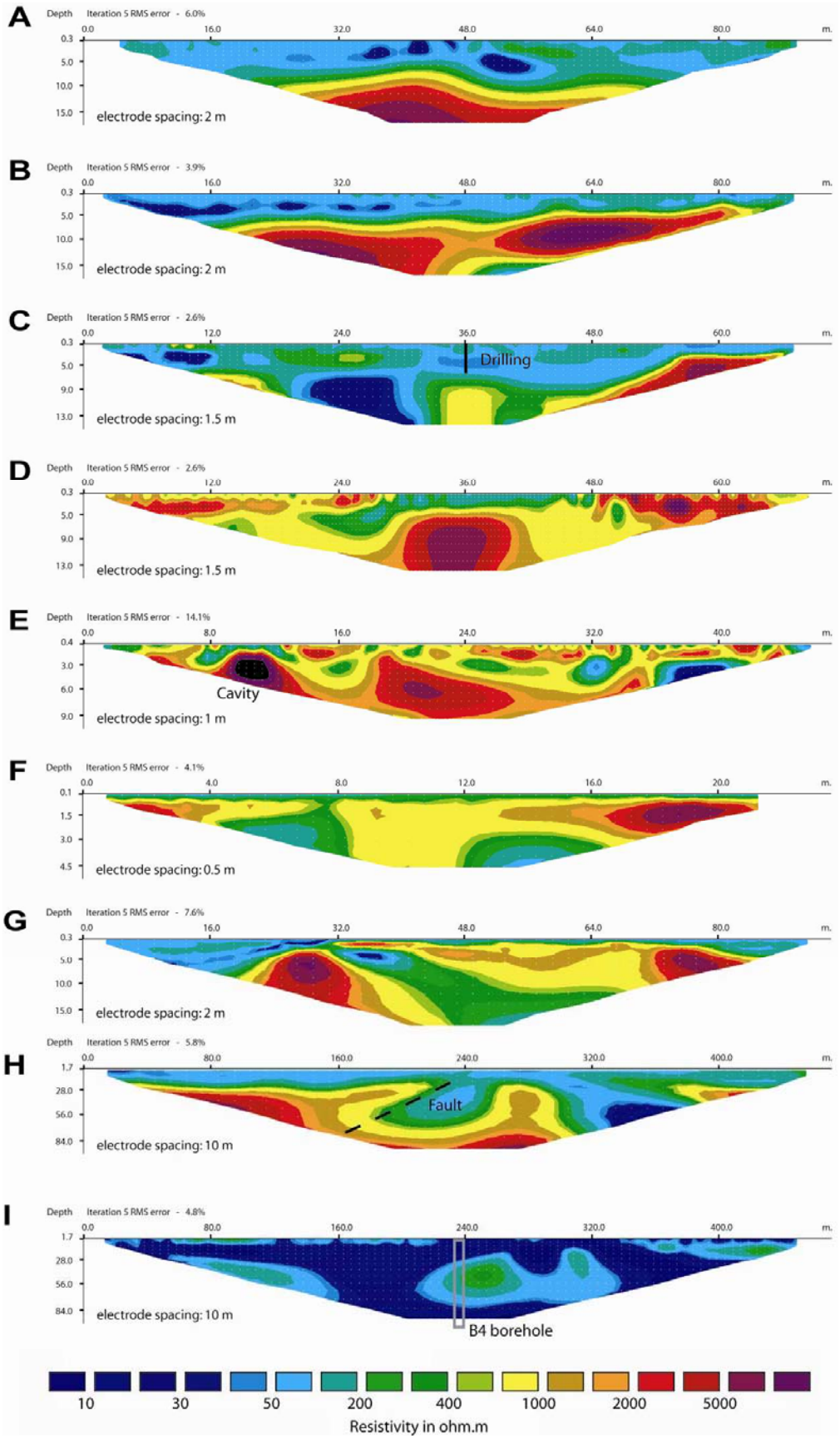

Figure 4.18: Inverted data of the electrical resistivity tomography lines for the different areas studied (the location of the profiles is showed in figure 4.16).

bounded to the one of anhydrite, so that zone has been interpreted to correspond to a less pure anhydrite rock.

Profiles D and E have been measured in other places in which anhydrite had stopped the exploitation of the quarry. The electrodes were nailed almost directly on the sulphate rocks and both anhydrite and gypsum appeared in the ground surface. In both inverted resistivity sections (figure 4.18, D and E) there is displayed a lateral variation of electrical resistivity ranging from 10^3 to 10^4 ohm.m. The larger resistivity values are bounded to the outcropping of massive anhydrite while the lower ones are related to the presence of gypsum; the intermediate values correspond to the transition of both sulphate phases. In the profile E the inversion calculate a very resistive body (more than $3x10^4$ohm.m) which probably corresponds to a cavity, usual in sulphate rocks.

The profiles F and G have been performed in abandoned quarries near to the village of Odena where anhydrite outcrops (figure 4.17G). The inverted section shows electrical resistivity ranging from 10^3 to 10^4 ohm.m; similarly to what has been observed in the quarry of Beuda. In the areas in which the value is larger massive anhydrite is observed. Lower electrical resistivity than 500 ohm.m are related to lutitic sedimentary layers.

The profiles H and I have been performed in no-outcropping evaporitical basins. The inversion of the H profile (figure 4.18F) displays a shallow deposit with low electrical resistivity value (50 ohm.m) which corresponds with the underlying materials. Below this layer there is a high resistivity body ranging from 1000 to more than 5000 ohm.m and with a more conductive structure in the center part (between 100 and 200 ohm.m). This structure represents a fault present in the area and identified in surface with geological evidences (Carrillo 2009). The profile I performed in Montes de Torrero area (figure 4.18I) the whole deposit shows a general trend of 30-50 ohm.m with some bodies slightly more resistive (until 300 ohm.m in the most resistive point). Those bodies would represent a higher purity of the deposit (up to 60% in purity in sulphates) in these zones, this purity changes are related to primary depositional processes and they are very common in these materials. In any case it is not possible to differentiate between anhydrite and gypsum layers because the electrical behavior of the deposit is dominated by the abundant matrix.

As general trend, anhydrite rocks with high purity show an electrical resistivity value of 10^4 ohm.m after the inversion. This value is considered to be interpreted as reference for pure anhydrite rocks because in some profiles in which some of the shallowest points have been

measured almost directly above massive anhydrite rocks, show an apparent resistivity value close to 5000 ohm.m. In these cases the apparent and the inverted resistivities are similar but a little bit lower for the apparent one because the electrodes are nailed on a thin clay layer. When these rocks are mixed with gypsum forming pure sulphate rocks, which are the most common ones in the quarries, display an intermediate value of resistivity ranging from 1500 to 5000 ohm.m depending the quantity of each phase. As the distribution of the anhydrite in the gypsum deposits is very heterogeneous due to the rehydration processes, the tomography lines show heterogeneous bodies with different electrical resistivity values and transitional zones. Values close to 1000 ohm.m are related to the purest gypsum rocks or to pure anhydrite with a significant quantity of matrix rocks. When the presence of matrix is large, there is no possibility of differencing gypsum from anhydrite with ERT.

.2.3 Laboratory essays

.2.3.1 Materials and methods

Following the same methodology, parameters and resources used in the elaboration of the gypsum-lutite pills eleven anhydrite-lutite pills have been elaborated. The aim of these measures is to observe the electrical resistivity trend of the anhydrite rocks in comparison with the trend showed in the case of gypsum rocks.

In addition, 12 pure monocrystal gypsum sheets have been obtained in order to observe possible electrical conductivity differences. The electrical conductivity of different mineral crystals has been already measured previously by many authors (Telkes 1950; Bleaney and Bleaney 1976; Keller 1966; Tomioka et al. 1998; Halpern 1998; Zou et al. 2009; among others). It is hard to obtain anhydrite crystals large enough as to perform these essays on them, so gypsum crystals have been used. From the sheets, 6 have been cut parallel and 6 cut perpendicular to the main exfoliation planes. The gypsum crystals tend to break along these exfoliation planes so in order to cut the sheets perpendicularly to this structure; the crystal has been previously embedded within a non conductive poliester resin (Norsodyne ref.9944). Anhydrite crystals are expected to have a similar resistivity to the sheets cut perpendicularly to the main exfoliation because the water molecules (only present in gypsum) are disposed in the other plane. The thickness of crystal samples has been measured with a vernier caliper.

The measure of conductivity has been carried out in accordance with the UNE 21-303-33 regulation (1983) with the same electrical circuit used in the case of gypsum pills (figure 4.19A). In order to measure the amperage of the electrical current after traversing the resistance (the sample), a micro-ammenter or a nano-ammeter has been used as well.

In the case of crystal sheets, the electrodes have been elaborated sticking insulating tape defining a rectangular tape-free surface in which an electrically conductive gel (Compex gel for ultrasonic transmission and electrostimulation) has been poured; spreading along the surface of the electrode. The two poles of the circuit cable are connected to the gel in both sides of the samples by foil grasped to copper clamps (figure 4.19B). The electrical current run by the gel surface and crosses the sample perpendicularly to it. This is due to the fact of that

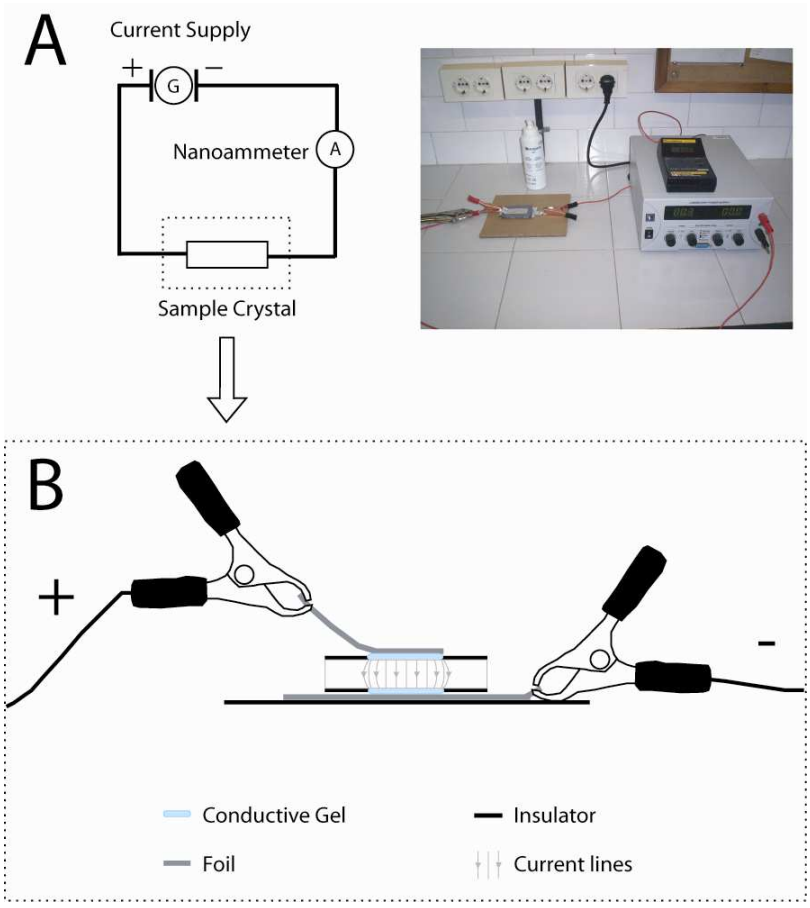

Figure 4.19: Electrical device to measure the electrical resistivity values of the samples; it consists of a switchable laboratory power-supply, two electrodes and an ammeter (micro or nano-ammeter depending on the samples). A) general scheme and sketch of the circuit; B) Electrode disposition for measures in crystal sheet samples, where the electric contact is made with conductive gel in a surface delimited with insulating tape.

the current tends to seek the most conductive way to spread, and the opposite gel electrode is the most conductive body towards which be directed; so the lateral leakages can be despised.

The crystal sheet and the electrode assemblage are situated above a paperboard insulator in order to prevent possible leakages. The measures have been taken switching on the power supply and waiting few seconds until the reading stabilizes (10 seconds); after a time the sample start to be polarized and the reading tend to increase. The longest time measures are not considered representatives for geophysical surveys because geoelectrical methods use a short current injection time. The resistivity (or conductivity) can be calculated from Ohm's law as in the case of gypsum pills.

The laboratory essays in crystal sheets have been carried out 5 times and the average value has been selected as the representative one. The selected voltage is 1V for exfoliation parallel cut sheets and 0.1V for exfoliation perpendicularly cut sheets (*a* and *b* directions respectively in figure 4.20). The selection of 1V in the case of samples parallel to the exfoliation planes is due to that there is no reading with 0.1V. The size of the electrode and the width of the sheet depend on the limitations of each crystal. Crystal sheets with impurities have been discarded to avoid conducting channels not related to the crystalline structure. An electrical resistivity test has been previously performed on the resin (0.3cm-thick resin sample with a 6cm^2 electrode, at 32.2 V) to prove its not conductive nature.

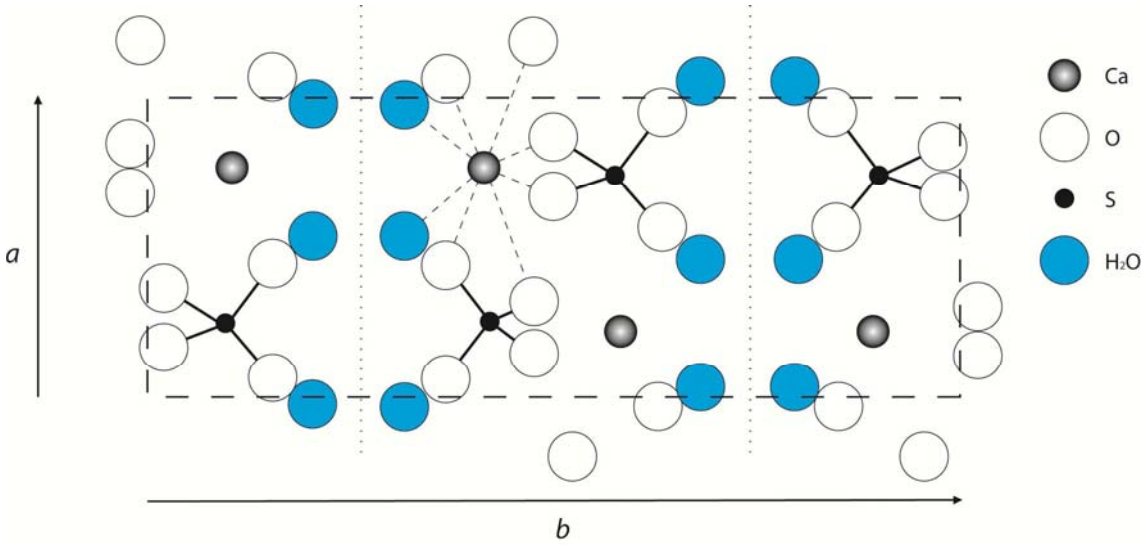

Figure 4.20: Crystallographic structure of gypsum, (a) and (b) are the main crystallographic axis (modified from Klein and Hulburt 1998).

.2.3.2 Results and discussion

The new measures performed in anhydrite-lutite pills have shown a similar trend to the one presented by gypsum pills. The pills ranging from 0 to 50% in anhydrite purity (Pa1 to Pa6; table 4.5) display a very scarce increasing trend of the electrical resistivity value (from 6 to 21 ohm.m). The pills ranged from 80 to 100% in anhydrite purity (Pa9 to Pa11; table 4.5) where out of scale of the microammeter and therefore they were measured with the nanoammeter showing higher electrical resistivity values (from $1.87x10^3$ to $1.35x10^4$ ohm.m). The 60 and 70% anhydrite purity pills (Pa7 and Pa8; table 4.5) display a transitional range of values of 44 and 279 ohm.m respectively. Comparing the trends of gypsum and anhydrite pills (figure 4.21) it is evident that the purities below 60% are dominated by the lutitic matrix and the sulphate component affects negligibly to the measure. The purities above 70% show high resistivity values in which the dominant component is the sulphate phase. Between the two differentiated trends there is a transitional zone which represents the loose of the connectivity of the matrix. As in the measures of gypsum pills, the pills with large quantity of clay component polarize with measuring time.

Sample	% Sulphate	Thickness (cm)	Voltage (V)	Measure (μA)	Resistivity (ohm.m)
Pa1	0	0.455	1.5	96	6
Pa2	10	0.470	1.5	78	7
Pa3	20	0.475	1.5	62	9
Pa4	30	0.490	1.5	48	11
Pa5	40	0.490	1.5	34	16
Pa6	50	0.490	1.5	26	21
Pa7	60	0.500	1.5	12	44
Pa8	70	0.520	0.1	0.122	279
Pa9	80	0.540	1	0.175	1870
Pa10	90	0.530	1	0.074	4505
Pa11	100	0.505	1	0.026	13457

Table 4.5: Results of the laboratory measures in the synthetic pills made of a mixing of powdered pure anhydrite or gypsum reagents and clay. The samples with larger purities in anhydrite (Pa7, Pa8, Pa9 and Pa10) have been measured with a nano-ammeter instead of a micro-ammeter.

Any combination of gypsum and anhydrite, when the presence of matrix is above 40%, will not affect the electrical resistivity value of the whole rock. This is due to that the matrix is

percolant and both gypsum and anhydrite act as non conductors and then the electrical current do not spread through them. This is bond to the high contrast between the conductivity of the sulphate phases and the matrix.

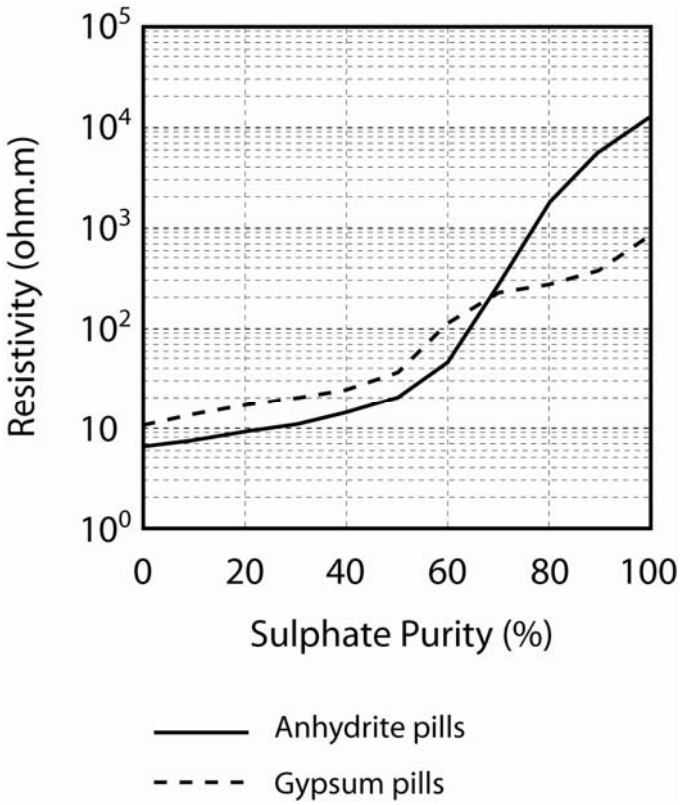

Figure 4.21: Semi-logarithmic plot representing the results of the measures in anhydrite-clay pills and compared to the results obtained for gypsum-clay pills.

In addition to the presence of matrix, the difference in the chemical composition between gypsum and anhydrite minerals is the presence of structural water within the crystal structure of the first one. This water forms molecular sheets which generates the main exfoliation planes (010) of gypsum crystals. The measures carried out upon gypsum crystals in different crystallographic directions display a clear difference between them (table 4.6). Crystal samples measured perpendicularly to the principal exfoliation planes (samples A1 to A6; table 4.6) have $1.5x10^{11}$ ohm.m with a standard deviation of 64%. The and samples measures parallel to the plane (010) (samples B1 to B6; table 4.6) show a maximum standard deviation of 20.9 nA and the mean electrical resistivity of the 6 samples is $8.9x10^{8}$ ohm.m with

a standard deviation of 31%. The resistivity ratio A/B is 169.7 meaning that the difference of resistivity is at least 2 orders of magnitude larger.

Sample	Thickness (cm)	Electrode area (cm2)	Voltage (V)	Essay 1 (nA)	Essay 2 (nA)	Essay 3 (nA)	Essay 4 (nA)	Essay 5 (nA)	Mean resistivity (ohm.m)
A1	0.125	3.00	1	21	25	11	17	13	1.40E+11
A2	0.100	2.90	1	10	7	9	13	11	2.90E+11
A3	0.070	3.00	1	28	7	16	15	21	2.50E+11
A4	0.080	0.80	1	19	22	34	37	17	3.90E+10
A5	0.050	1.05	1	37	8	17	22	13	1.10E+11
A6	0.040	0.98	1	14	44	32	34	22	8.30E+10
B1	0.415	2.16	0.1	74	81	83	73	66	6.90E+08
B2	0.575	3.22	0.1	49	68	42	95	54	9.10E+08
B3	0.635	3.08	0.1	38	52	60	72	36	9.40E+08
B4	0.360	3.75	0.1	78	82	61	106	48	1.40E+09
B5	0.375	1.60	0.1	39	66	52	70	61	7.40E+08
B6	0.490	2.00	0.1	48	59	64	54	83	6.60E+08

Table 4.6: Result of the laboratory measures in crystal sheets. A samples are cut parallel to the main exfoliation planes (010) and B samples are perpendicularly to them.

Besides, both set of samples polarize in longtime measures; meaning that in addition to the clay components gypsum crystals also polarize. The B samples polarize more rapidly and because of that, the electrical current runs more easily. In the plane (010) the water molecules form exfoliation planes in which the hydrogen atoms create a positive electric field. This is due to that the oxygen atoms of water molecules are oriented towards to the calcium atoms of the crystalline structure while one of the hydrogen atoms of each water molecules is oriented towards to a sulphate related oxygen in the opposite part of the crystalline structure forming a weak ionic bound (figure 4.22A).These planes with feeble electric field facilitate the pass of electrical current in that direction.

It is difficult to obtain an anhydrite crystal larger enough to perform electrical resistivity measures; because of this no measures have been performed in anhydrite. In any case anhydrite lacks of the exfoliation planes formed by water molecules and then it is expectable that its electrical resistivity value is larger than the one of gypsum (figure 4.22B). Both gypsum and anhydrite show other exfoliation structures with preferential directions different than the principal. In the case of anhydrite the main exfoliation planes are (010), but these planes are defined by different covalent bound length of the calcium atoms with its surrounding oxygen ones. These planes do not generate such electric field as in the case of the water-related exfoliation system.

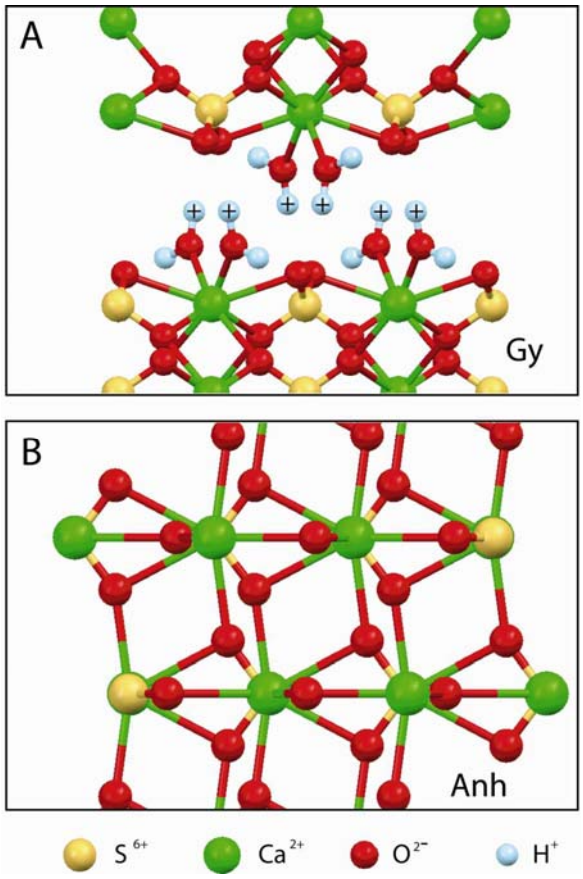

Figure 4.22: A) Detail of the atom and charge distribution in the water layers of gypsum crystals displayed in figure 4.20 (the crystallographic axis are turned 90º); B) crystallographic structure of anhydrite.

.2.4. Theoretical calculations

.2.4.2 Hashin-Shtrikman bounds for three-phase systems

In the case of anhydrite rocks is expectable to obtain the same trend observed in the case of gypsum rocks (figure 4.23), this is, values similar to the lower bound when the rock purity is under 60% and similar to the upper bound when the purity is above 70%; with a transition between 60 and 70%. As in the case of gypsum, if the matrix is percolant, the resistivity in conditioned by its value and when it is not percolant, is conditioned by the anhydrite phase, which acts as a dielectric.

The electrical resistivity value selected for pure anhydrite phase has been 10^4 ohm.m, in accordance with the maximum value measured in field examples and the bibliography. The

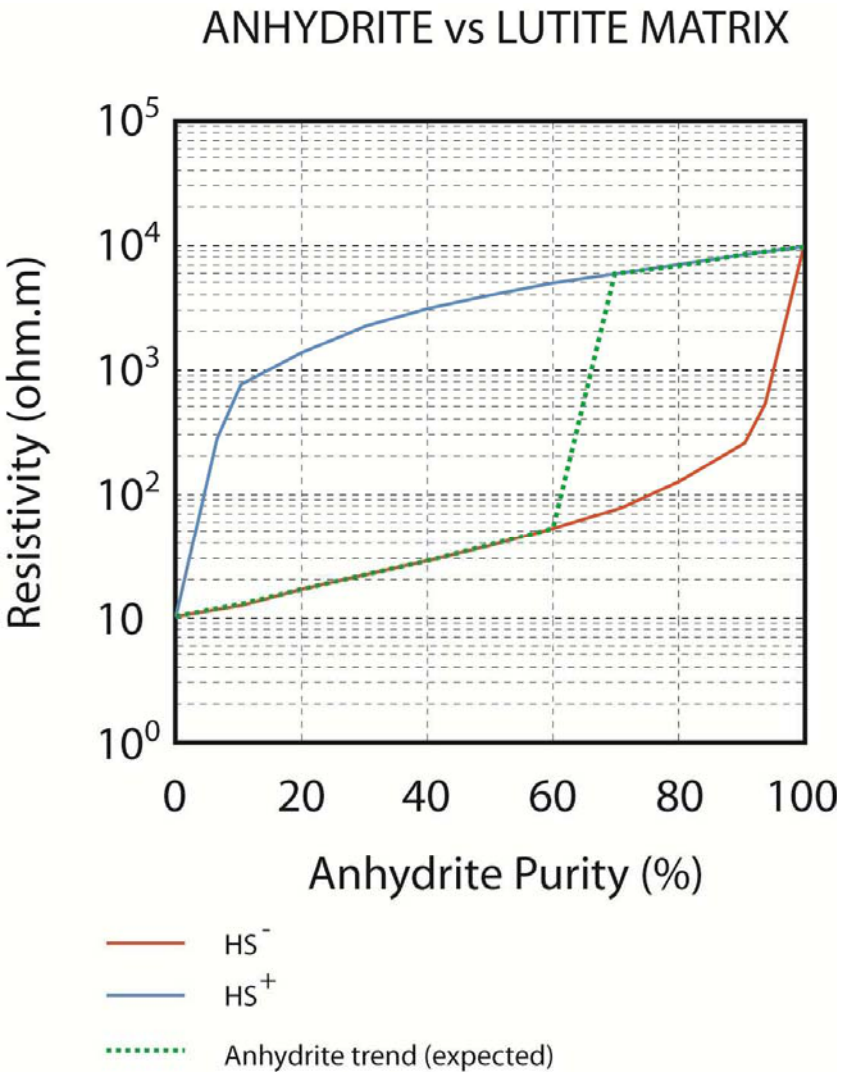

Figure 4.23: Hashin-Shtrikman bounds for anhydrite-lutite system and the expected trend of electrical resistivity value considering the percolation phenomena observed in the laboratory essays.

trend has been supported by the results of the laboratory measures in pills and the field measures with ERT. In the case of anhydrite, often appears in association with gypsum, so a binary system of anhydrite and lutite is not enough to describe its electrical behavior. A general form of the bounds for n-phases was given by Berriman (1995). With his formulae it is possible to elaborate ternary graphics for 3-phased rocks (Ledo and Jones, 2005). Gypsum-Anhydrite-Lutite (GAL) system has been calculated for both upper (HS^+, equation 5) and lower (HS^-, equation 6) HS bounds:

Equation 4.5: $$\rho_{HS^+}{}_{gy,anh,lu} = \frac{1}{\left(\frac{\gamma_{gy}}{\rho_{gy}+2\rho_{lu}}\right)+\left(\frac{\gamma_{lu}}{3\rho_{lu}}\right)+\left(\frac{\gamma_{anh}}{\rho_{anh}+2\rho_{lu}}\right)} - 2\rho_{lu}$$

Equation 4.6: $$\rho_{HS^-}{}_{gy,anh,lu} = \frac{1}{\left(\frac{\gamma_{gy}}{\rho_{gy}+2\rho_{anh}}\right)+\left(\frac{\gamma_{lu}}{\rho_{lu}+2\rho_{anh}}\right)+\left(\frac{\gamma_{anh}}{3\rho_{anh}}\right)} - 2\rho_{anh}$$

In the case of lower bound (figure 4.24A), the system is clearly dominated by the lutitic component; the isoresistivity lines are parallel between them showing no appreciable variation in the gypsum-anhydrite axis but when the lutite component is less than 10%. The values of resistivity are very low in general showing less than 100 ohm.m for sulphate purity of 70%. The upper bound (figure 4.24B) displays a very different trend dominated by the anhydrite component, but in this case the 3 components affect the bulk resistivity value of the rock. The electrical resistivity values are much larger than in the case of lower bound achieving 1000 ohm.m with only 40% of anhydrite. As it has been previously shown, the electrical behavior of the rocks is the one of lower HS bound when the quantity of matrix is above 40% and the one of upper bound when is below 30%. Thus it is expectable that the real distribution of the electrical resistivity for the GAL system should be a combination between the upper and lower HS bounds (figure 4.24C).

.2.4.1 Conductivity calculation: methods

The effective properties of composites, in particular electrical conductivity, have been studied analytically for a long time for a very simple cases (i.e Maxwell calculated the effect that a single spherical inclusion, with a different conductivity from the matrix). The rocks can be considered as random materials of different property phases at various length scales. To compute the effective properties of such materials requires knowledge of the microstructure and require numerical computation. Garboczi (1999) wrote an algorithm and the consequent FORTRAN code to computed using finite difference and finite elements electrical an elastic effectives properties from a digital images of a material composed of different phases.

In this paper we have used the program ELECFEM2D.F from Garboczi to compute the effective conductivity of gypsum-anhydrite rock samples. The method to calculate the electrical conductivity value of these rocks is to analyze thin section images in which the amount of both anhydrite and gypsum proportion together with the one of the lutitic matrix is known. With this software it is possible to elaborate a resistivity distribution model based on a photograph.

In order to perform the theoretical calculation of photographs with the program ELECFEM2D.F, the pictures must be converted from HTML format (either JPG, JPEG, GIF, PNG

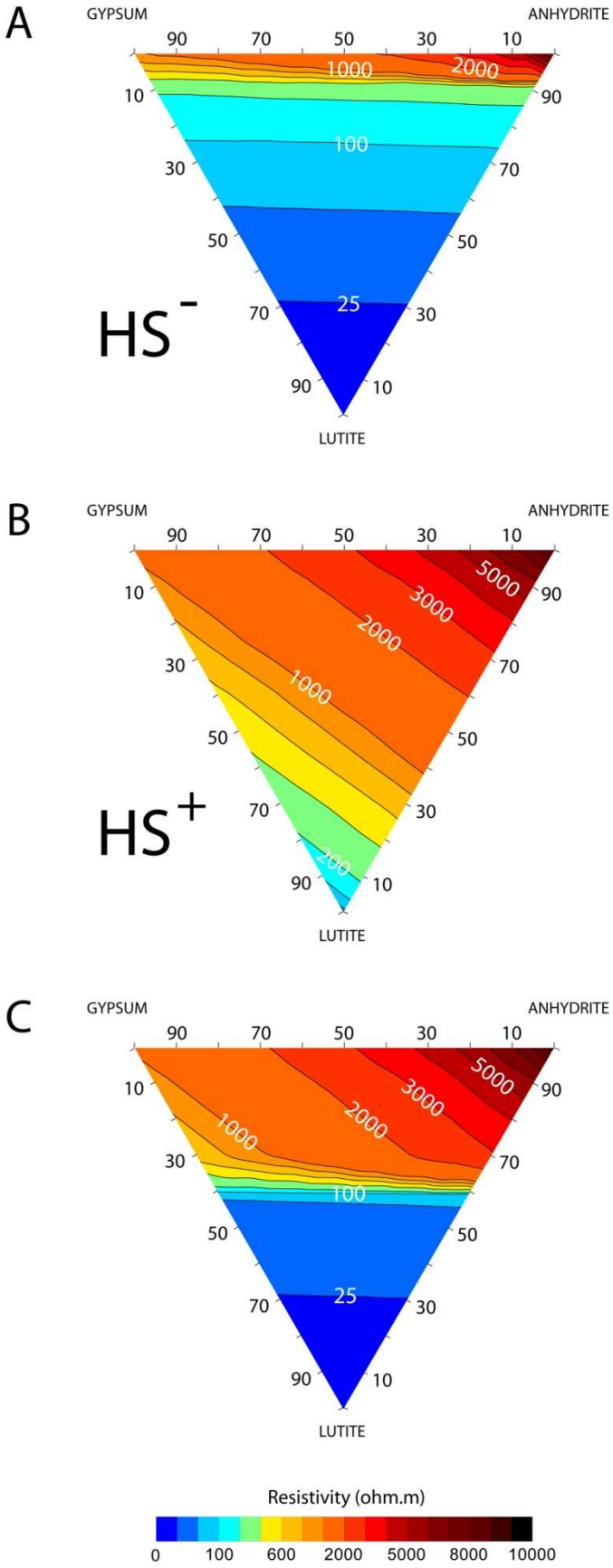

Figure 4.24: Ternary plots showing Hashin-Shtrikman bounds for gypsum-anhydrite-lutite (GAL) system. A) lower HS bound; B) upper HS bound; C) combined diagram considering the percolation phenomena.

or other image format file) into ASCII. This has been carried out with a converter which creates numerical files from the pixels of the input image. Depending on the color range of these pixels, a numeric value which is related to a user defined electrical resistivity value is assigned (figure 4.23). As the images used display lutite, gypsum and anhydrite phases; 10, 10^3 and 10^4 ohm.m electrical resistivity values have been selected respectively. The number of variables is user defined and 2 variables (1 and 2) have been selected for photographs displaying 2 phases (any couple of lutite-gypsum-anhydrite) and 3 variables (1, 2 and 3) when the 3 of them are present. The more the color variables there are, the harder is their identification; so to improve the detection of each phase by the HTML/ASCII converter, each image has been treated with an image processing program in order to homogenize the color ranges.

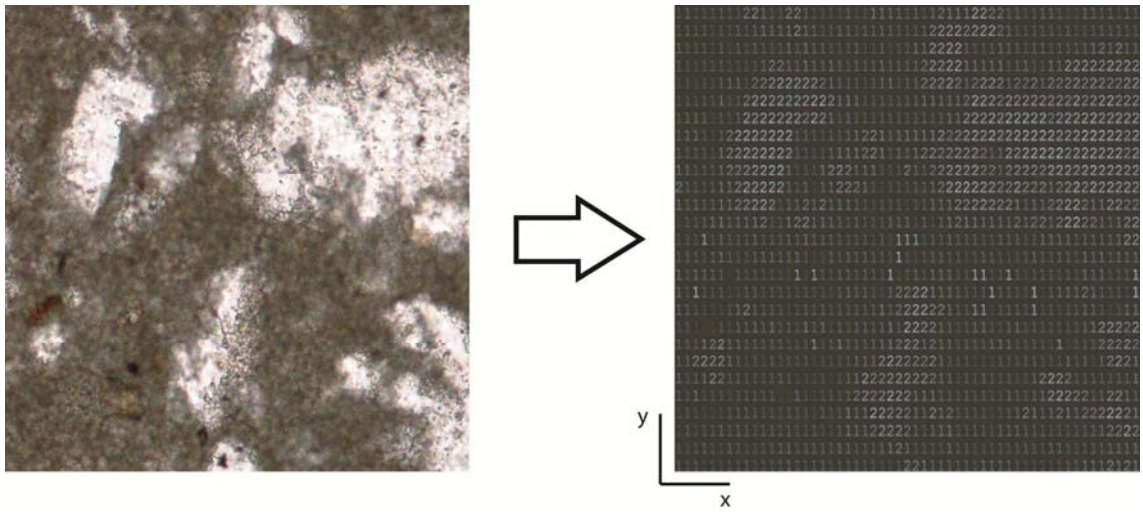

Figure 4.25: Graphical display of the HTML/ASCII conversion process. 2 numbers corresponds to gypsum phase and 1 numbers to matrix in the ASCII one.

Once the ASCII file is created, it can be run into the ELECFEM2D.F program. The ASCII files used have 150 columns and 56 rows and before being read by the program they have to be converted in a single column file. The program divides the surface into 8400 (150x56) cells with an electrical resistivity value assigned to each one and calculates the current intensity remaining after crossing the system in *x* or *y* direction. Both directions and the mean value have been calculated; the differences are related to the anisotropic distribution of the phases. The selected current has been 1 V/m, but other current intensities have been tried without altering the result.

.2.4.3 Conductivity calculation: results and discussion

In order to check the accurateness of this GAL diagram, the theoretical electrical resistivity value of real thin section rock photographs (figure 4.26) has been calculated with ELECFEM2D program. Lutitic matrix display brownish coloring while both anhydrite and gypsum have are transparent underplane polarized light; having anhydrite higher relief than gypsum (its bounds are well marked with dark lines). With crossed polarized light, gypsum and anhydrite can be easily differentiated because of the different coloring of the anhydrite (pink, green, blue, …) in contrast with the gray colors of the gypsum crystals. The standard electrical resistivity values selected for the gypsum, anhydrite and lutitic matrix phases have been 10^3, 10^4 and 10 ohm.m respectively, as has been assigned before. The electrical resistivity of the bulk sections has been measured in both *x* and *y* directions; when the distribution of the components is homogeneous these values would be considered similar. For each thin section the fractions of the components are calculated by the program so it is possible to obtain the electrical resistivity value corresponding to these fractions calculated with Hashin-Shtrikman bounds (table 4.7).

The results show that the mean of the calculated electrical resistivity values in *x* and *y* directions are in general close to HS^+ bound when the quantity matrix is lower than 30% (figure 4.26, thin sections A, D, E, F, G and H; table 4.7) and to the HS^- bound when the quantity of matrix is abundant (figure 4.26, B and I; table 4.7). There is a good match between the corresponding position of each sample in the figure 4.25C, according to their components percentages, and the calculated resistivity values. In the case of thin sections C and J there there is abundant matrix (58 and 52% respectively); nevertheless, the calculated resistivity values are slightly larger than that expected for such mixture.

This is due to that the phases are not scattered and randomly distributed within the samples but forming compact and pure areas. This represents large heterogeneities which change the percolating behavior (we have considered it only for regular distributions of the phases as in the case of the pills) of the bulk rock and makes the transition zone larger. In any case the values are always much closer to the lower bound that to the upper one. At larger scale (as in the field examples) the rocks are in general more homogeneous and should fit to the HS lower bound for compositions of 40-60% in lutitic matrix; even it is also possible to have this effect if there are heterogeneities at greater scale.

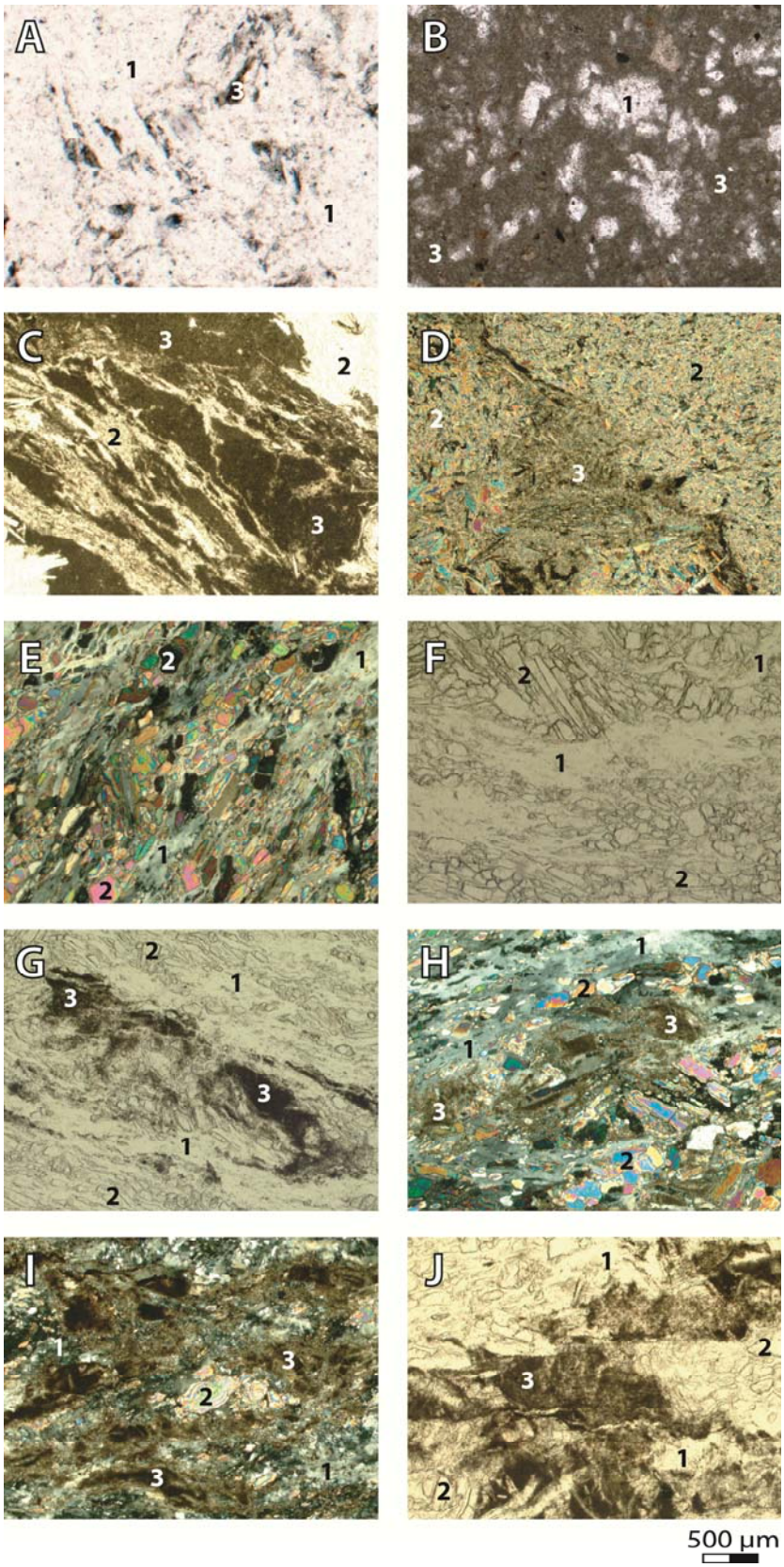

Figure 4.26: Microphotographs of thin section of calcium sulphate rocks. D, E, H and I are taken with cross polarized light and the rest with plane polarized light. The different phases are indicated with numbers 1 (gypsum), 2 (anhydrite) and 3 (lutite/carbonate).

Thin section	%Gy	%Anh	%Lut	HS- (ohm.m)	HS+ (ohm.m)	X (ohm.m)	Y (ohm.m)	Mean (ohm.m)
A	95	0	5	365	928	862	844	853
B	17	0	83	16	129	16	16	16
C	0	42	58	32	1091	214	126	170
D	0	83	17	154	4504	3087	3157	3122
E	29	71	0	2796	4417	5070	6024	5547
F	68	32	0	1411	1947	1622	2265	1944
G	26	51	23	105	2105	1102	2474	1788
H	53	34	13	185	1708	1129	1940	1535
I	35	6	59	30	408	33	82	58
J	38	10	52	36	540	65	210	138

Table 4.7: Results of the theoretical calculations of electrical resistivity of the thin section photographs with ELECFEM2D software. The result of the measures in both x and y directions as well as the mean resistivity values are listed. Lower (HS^-) and upper (HS^+) Hashin-Shtrikman bounds have been also calculated, only considering the proportion of each phase. The corresponding image of the thin sections A to J are displayed in the figure 4.26.

.2.5 Geoelectrical classification of sulphate rocks

With the GAL diagram obtained combining both HS^+ and HS^- boundaries for a gypsum anhydrite-lutite system (figure 4.25C) a geoelectrical classification has been elaborated differentiating 6 calcium sulphate rock types (figure 4.27). When the lutitic matrix is connected at long range (in the case of sulphate purity lower than 60%) the system is matrix dominant and therefore there is no possibility of differentiating between gypsum and anhydrite component; these rocks are classified as Lutites and Gypsum/Anhydrite rich Lutites. The electrical resistivity of this groups range from 10 to 100 ohm.m. When the sulphate purity is larger than 70%, the rock will be considered as Pure Gypsum when it ranges from 700 to 1000 ohm.m as has been previously stated in the geoelectrical classification of gypsum rocks. If the sulphate mineral is mainly anhydrite (more than 90%) the rock is considered Pure Anhydrite and its electrical resistivity value range from 2500 to 10^4 ohm.m depending of the rock purity. In the case of presence of both gypsum and anhydrite sulphate phases, the rock is considered Gypsum with Anhydrite (1000 to 2000 ohm.m) or Anhydrite with Gypsum (2000 to 5000 ohm.m).

The values of pure Anhydrite and Anhydrite with Gypsum overlap; in this case it is possible to bond the electrical value to Pure Anhydrite rocks when there are no evidences of rehydration and to the Anhydrite with Gypsum in the contrary case. Between Lutites and

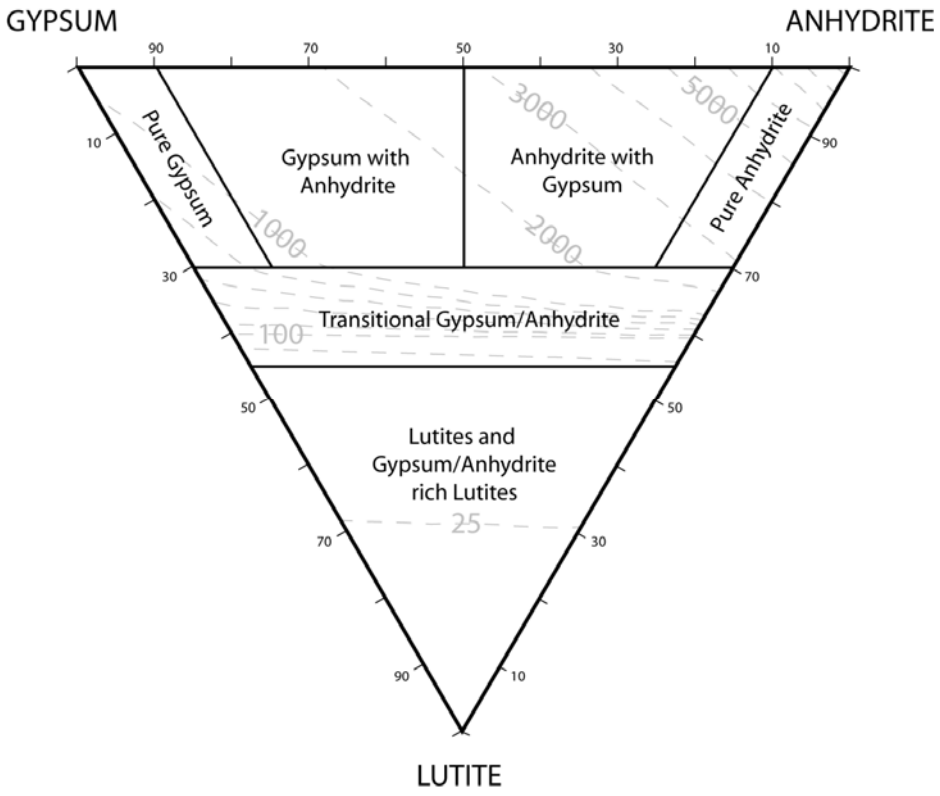

Figure 4.27: Geoelectrical classification of calcium sulphate rocks, depending on their gypsum-anhydrite-lutite contents. In the background is displayed in gray lines the resistivity value trend showed in figure 4.24C.

Gypsum/Anhydrite rich Lutites and the sulphate pure rocks there is a transitional area displaying transitional values from 100 to 700/2500 ohm.m (depending of the sulphate composition). The lower boundary of Transitional Gypsum/Anhydrite rocks has been selected for 55% in sulphate purity instead 60% because the measures in pills have shown that the 60% values display an electrical resistivity increasing trend; the upper boundary is 70% in gypsum purity.

.3 GLAUBERITE

.3.1 Introduction

Glauberite is a sedimentary mineral originated by evaporation processes. It is composed of sodium and calcium sulphate ($Na_2Ca[SO_4]_2$) what is usually associated with other sulphate minerals (thenardite, gypsum and/or anhydrite) and halite, and embedded within a clayly, marly or carbonatic (calcite, dolomite or magnesite) matrix. The mineral compositions and their relative abundance strongly vary from one glauberite deposit to another (Salvany 2009). After burial, glauberite deposits may experience uplift and are affected by surface and subsurface weathering processes. In this case, glauberite tends to become hydrated and to be replaced by gypsum (togheter with accompanying anhydrite).

An important episode of glauberite deposition took place in the Ebro, Tajo and Calatayud basins (Spain) during the Tertiary (Ortí and Salvany 1991; Ortí 2000; Ortí and Rosell 2000). Sodium sulphates were found in the Zaragoza formation during the construction of the high velocity train railways (AVE). A drilling campaign was performed by PROVODIT Engineering in the Montes the Torrero area (between 2002 and 2005) and glauberite rocks were found at depth. Glauberite deposits (together with gypsum, anhydrite and thenardite) are the currently exploited sulphate rocks for industrial purposes. Main glauberite producing countries are Mexico, Spain, USA, Canada and Iran. Glauberite is used mainly as component of powdered detergent for washing machines; but also in the industries of paper, glass, pharmacy, textile, to synthesize enzymes (to the elaboration of wine) among others.

The electrical resistivity value of glauberite rocks has not been previously studied. Although no references exist on this topic, it is supposed as an initial hypothesis that the expected resistivity values for glauberite rocks would be higher those of the gypsum ($CaSO_4 \cdot 2H_2O$), as in the case of the anhydrite ($CaSO_4$), which has larger electrical resistivity value due to the lack of water layers in his crystal structure. In the case of gypsum rocks, the electrical current spreads preferably along their crystallization water layers. As it has been showed before, the electrical resistivity of gypsum rocks is around 10^3 ohm.m (in case of high purity composition) while electrical resistivity of pure anhydrite is 10^4 ohm.m. In the case of calcium sulphate rocks, the influence of the presence of lutitic matrix (mainly clay and microcrystalline carbonates) in the electrical resistivity is as critical as in the case of calcium sulphates. Thus, when the quantity of matrix in the rock is larger than 45%, is connected at long range resulting in a percolant system. Because of this, the electrical resistivity of these

rocks is dominated by the value of the matrix displaying no differences for different sulphate compounds. The glauberite rocks have commonly large quantity of matrix so they are supposed to be affected by this phenomenon; it is rare to find high purity glauberite deposits, which should display high electrical resistivity values. A case of high purity glauberite layer has been studied in the Western part of the Ebro basin (La Rioja, Spain).

.3.2 Field data

.3.2.1 Materials and methods

A total of 6 ERT profiles have been performed in glauberite bearing evaporitical formations of the Ebro basin (Northeastern Spain; fig 4.28). 4 of them were carried out close to the city of Zaragoza (Zaragoza, Spain) and the other 2 ones in the surroundings of Alcanadre (La Rioja, Spain). All the profiles where performed in areas in which there was available information from boreholes crossing glauberite units in order to compare them with the electrical imaging.

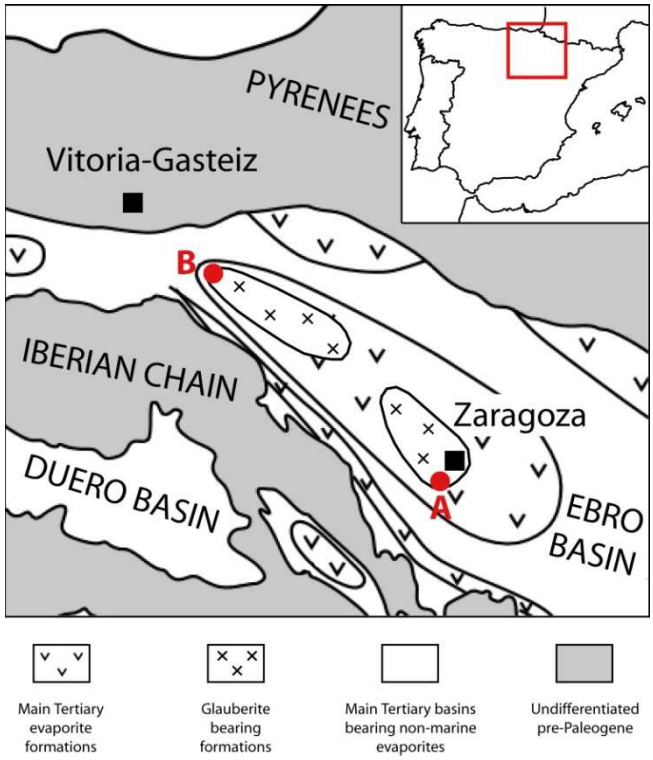

Figure 4.28: Main evaporitical basins of middle-North Spain. A and B are the two studies areas, Zaragoza and La Rioja sectors respectively (modified from Ortí et al. 2010).

In this study Wenner alpha, Wenner-Schlumberger and Dipole-Dipole arrays have been tried. Wenner-Schlumberger has been selected as the proper one because of his investigation depth and stability; in the case of Dipole-Dipole the data was very noisy in the areas with lateral topography variations. The resistivity-meter used for the data acquisition was Syscal Pro switch with 48 electrodes with 10 meter spacing between them and external power supply. The data was inverted with RES2DINV software.

Additionally to the ERT imaging, sulphate samples have been collected in some of the studied areas in order to evaluate the purity of the deposits. The rock samples have been powdered and afterwards 0.5g has been weighted and dissolved in 250 ml of distilled water. The solutions have been shaken during 24 hours. Thanks to the solubility of the sulphate minerals, these phases are dissolved in the distilled water so filtering the solution the residue left correspond with the non-soluble phases. This remnant represents the lutitic matrix (carbonates, quartz and other accessory minerals). Thus, the matrix can be weighted and quantified.

.3.2.2 Geological settings

The Ebro basin was developed during the Tertiary as the evolution of the foreland basin of the Pyrenee chain to an endorheic basin. A large evaporitical deposition took place during the Miocene (Ortí and Salvany 1991). In the Aragón sector of the Ebro basin there is an evaporitical sequence of hundreds meter thick, including several evaporate units. In the Miocene Gypsum and Anhydrite Zaragoza formation, anhydrite, glauberite and halite occur at depth (also thenardite in small quantities), while gypsum is the main evaporite mineral in exposed areas, as a consequence of hydration processes of the precursor anhydre sulphates; presence of marl and clay is ubiquitous. Salvany (2009) described 3 different units in this formation, from bottom to top: a) halite unit, up to 150 meters thick; b) glauberite-halite unit, with a thickness between 50 and 100 meters; c) anhydrite unit, hundreds of meters thick. The Montes de Torrero glauberite deposit corresponds to the glauberite-halite unit within the Gypsum and Anhydrite Zaragoza formation. In the studied area, the unit displays a monoclinal disposition, dipping up to 2º towards to the north. Minor folding and faulting is related to subsurface evaporite dissolution and collapse processes (Guerrero et al., 2003). This area has been studied by means of four ERT profiles situated close to the places where information from boreholes was available (figure 4.29A).

In the western part of the Ebro basin (La Rioja sector; figure 4.28) is situated the sulphate formation of Lerín Gypsum formation (Salvany and Ortí 1987), which is constituted of

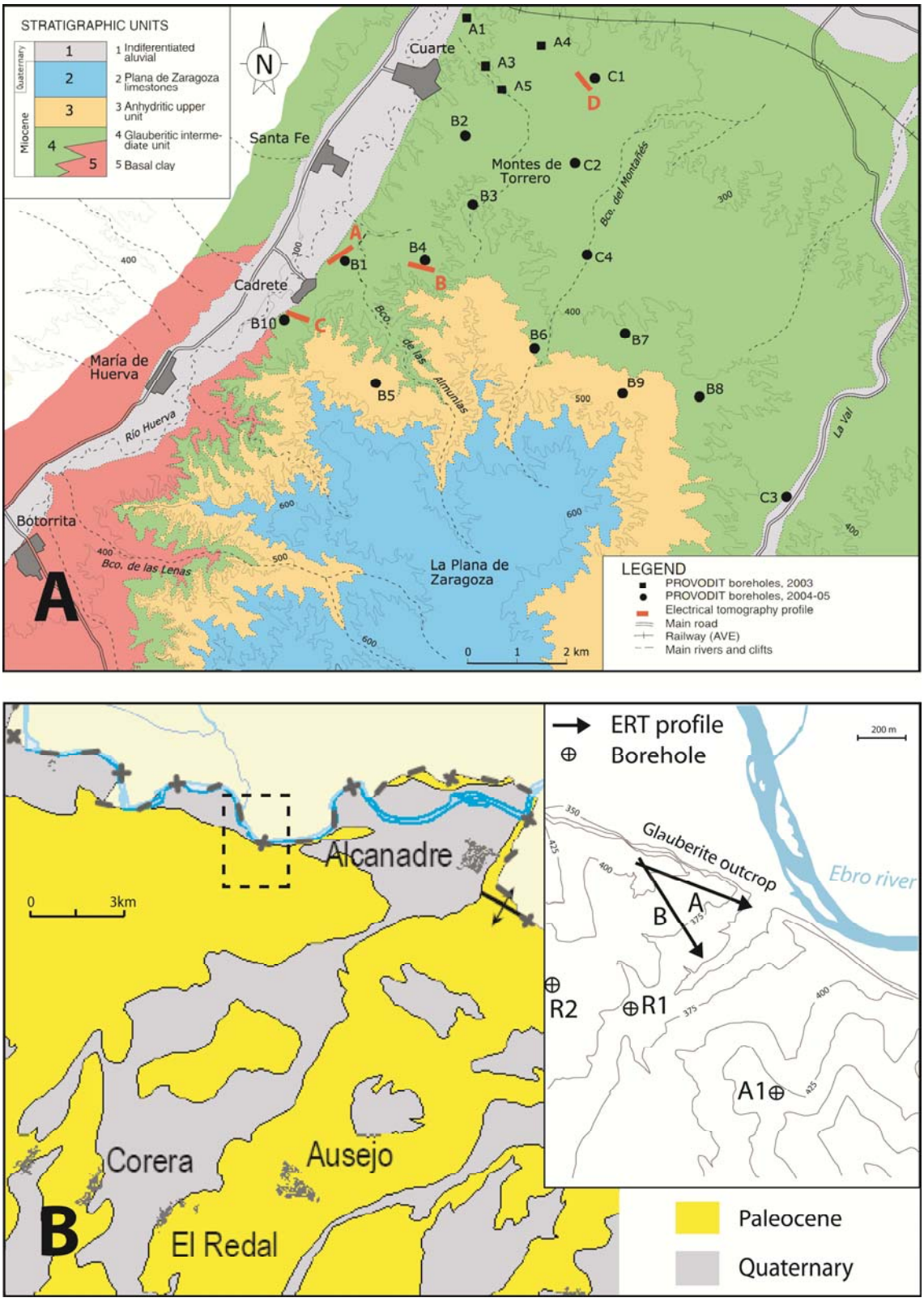

Figure 4.29: A) Detailed geological mapping of the Montes de Torrero area. A1 to C4 are the available drilling points, while A, B, C and D (in red) are the location of the performed ERT lines (modified form Salvany 2009). B) Geological mapping of the Alcanadre-Arrubal area; the studied area is marked with a dashed line. The topographic information of this area is displayed at the right part of the image (modified from the geologic map of Comunidad Autónoma de La Rioja 2009). Location of both areas in figure 4.28.

some nodular to laminated secondary gypsum levels alternate with lutite layers. In depth, the calcium sulphate is anhydrite. Other sulphate minerals as glauberite and thenardite are present in some of the evaporitic layers (gypsum, anhydrite). The area of Alcanadre-Arrúbal (figure 4.29B) was formerly exploited to obtain glauberite and these rocks appear at the base of the thick gypsum sequences of that unit. This deposit of glauberite rocks outcrop exceptionally due to the erosion generated by the adjacent Ebro River.

.3.3.3 Results and discussion

In the Montes de Torrero area, four ERT profiles have been carried out in accordance with the position of boreholes B1, B4, B10 and C1 (figure 4.29A). In these boreholes glauberite layers have been found at depth (figure 4.30). The profiles have been performed with the boreholes situated on their center with the exception of B10, which is situated on the western side and some few meters above the tomographic line.

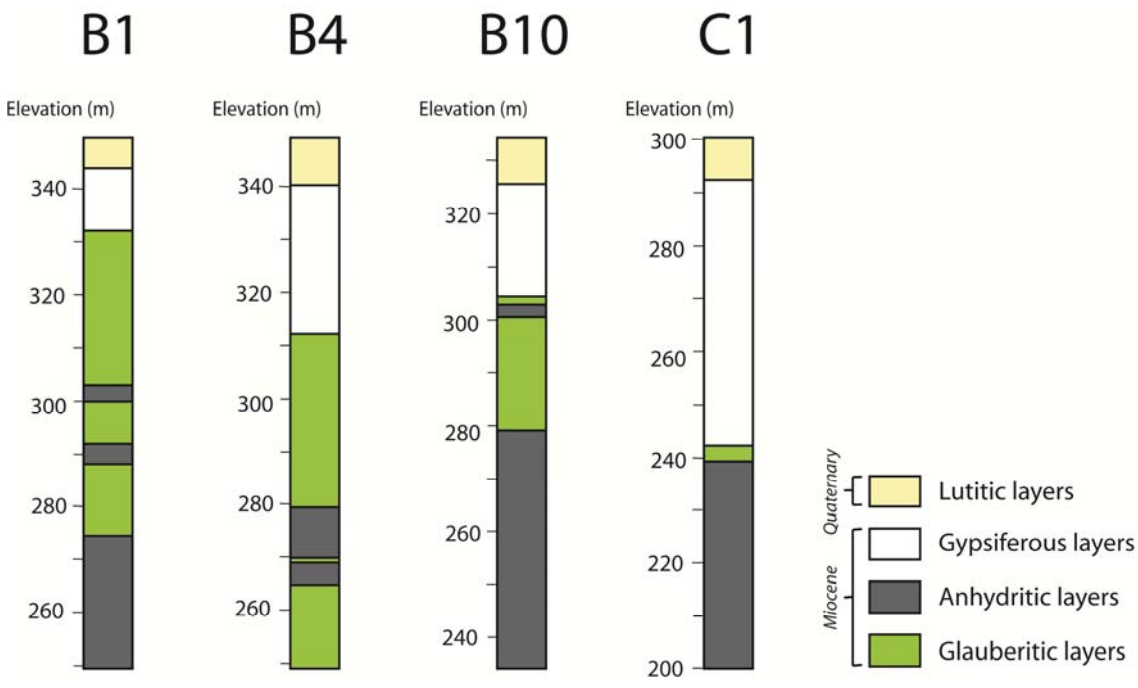

Figure 4.30: Synthetic representation of the boreholes B1, B4, B10 and C1 performed by PROVODIT Engineering in the Montes de Torrero area. The situation of the boreholes is displayed in figure 4.29A.

The outcropping materials in the area of B1 borehole (figure 4.31A) show a very impure composition of the sulphate rocks with a large quantity of matrix on them. The

inverted electrical resistivity profile (figure 4.32A) shows a general low resistivity trend with values below 50 ohm.m on it. The log of the borehole has a great quantity of matrix at any depth; similarly to outcropping rocks. There are some sulphate layers in which the amount of matrix is lower, but always above the 50% in composition (figure 4.33A). At a depth of 60 meters there is the purest layer of glauberite of the whole borehole and the purity of the rock in glauberite mineral is above 50%, but this is not shown in the profile. According with the electric percolation threshold of sulphate rocks described for the case of calcium sulphate rocks, the matrix in this whole area is percolant and so, the presence of different sulphate phases should not affect the electrical resistivity and then it is not possible to differentiate them.

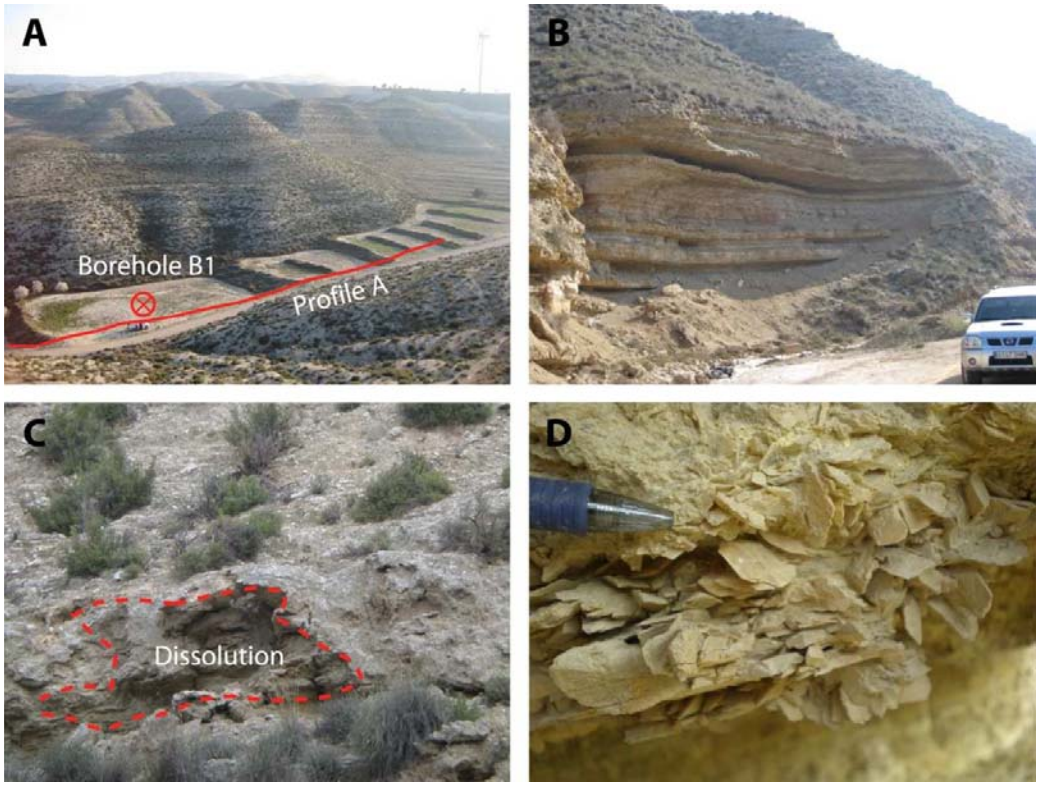

Figure 4.31: Photographs of the outcropping evaporitical units in the Montes de Torrero area (Zaragoza sector). A) General view of the region in the area of B1 borehole; B) View of layered-nodular gypsum-lutites sequence; C) Superficial dissolution processes (red dashed line); D) Detail of outcropping glauberite pseudomorphs (hydrated to secondary gypsum).

In the areas of the boreholes B4 and B10 there are evidences of dissolution processes (figure 4.31C) and the glauberite appears in surface as pseudomophs of gypsum (figure 4.31D).

The inverted profile of the B4 borehole (figure 4.32B) shows low resistivity values due to the low purity of the sulphate rocks of the terrain. Approximately at depth between 20 and 60 meters (depending on the position) the resistivity increases defining a laterally discontinuous structure. This structure is probably associated to changes in purity (figure 4.33B). B4 borehole has less matrix quantity below 40 meters depth; in accordance with the structure displayed in the profile. The lateral purity variation of this level is probably bounded to depositional primary processes, which are typical in sulphate rocks. The resistivity value of this structure (up to 300 ohm.m), indicates that it is at transitional composition ranging between 55 and 75%

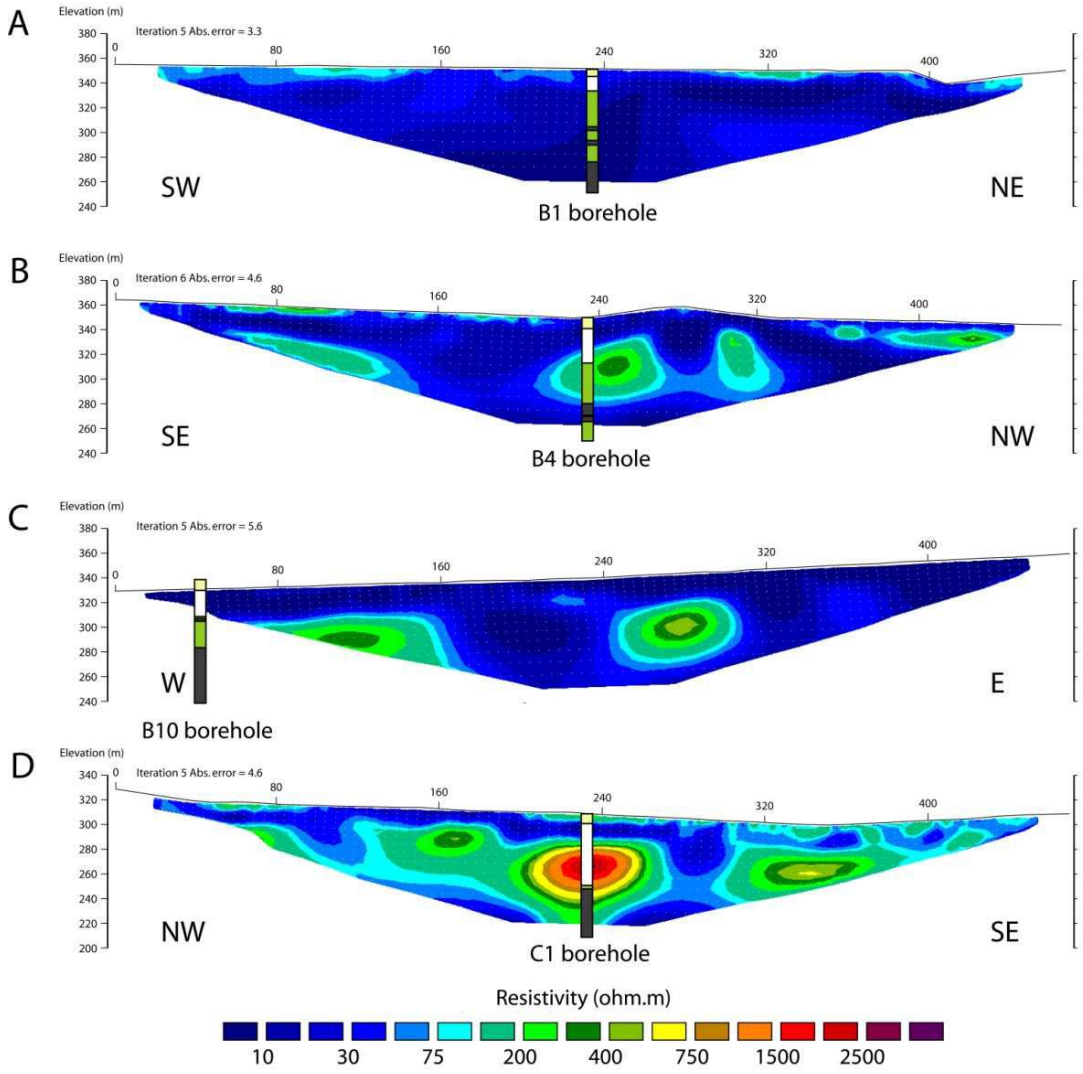

Figure 4.32: Inverted resistivity images of Montes de Torrero area. The synthesized borehole representation is superimposed to the profiles in their corresponding location. The situation of the profiles is showed in figure 4.29A. Legend of the lithologies of the boreholes in figure 4.30.

in sulphate purity. At the bottom, the resistivity turns to decrease again, meaning purity similar to the shallowest layers. This is also shown in the B4 borehole. The sharpest lateral resistivity changes (especially in the NW part of the profile), may be bounded to dissolution processes and posterior infilling.

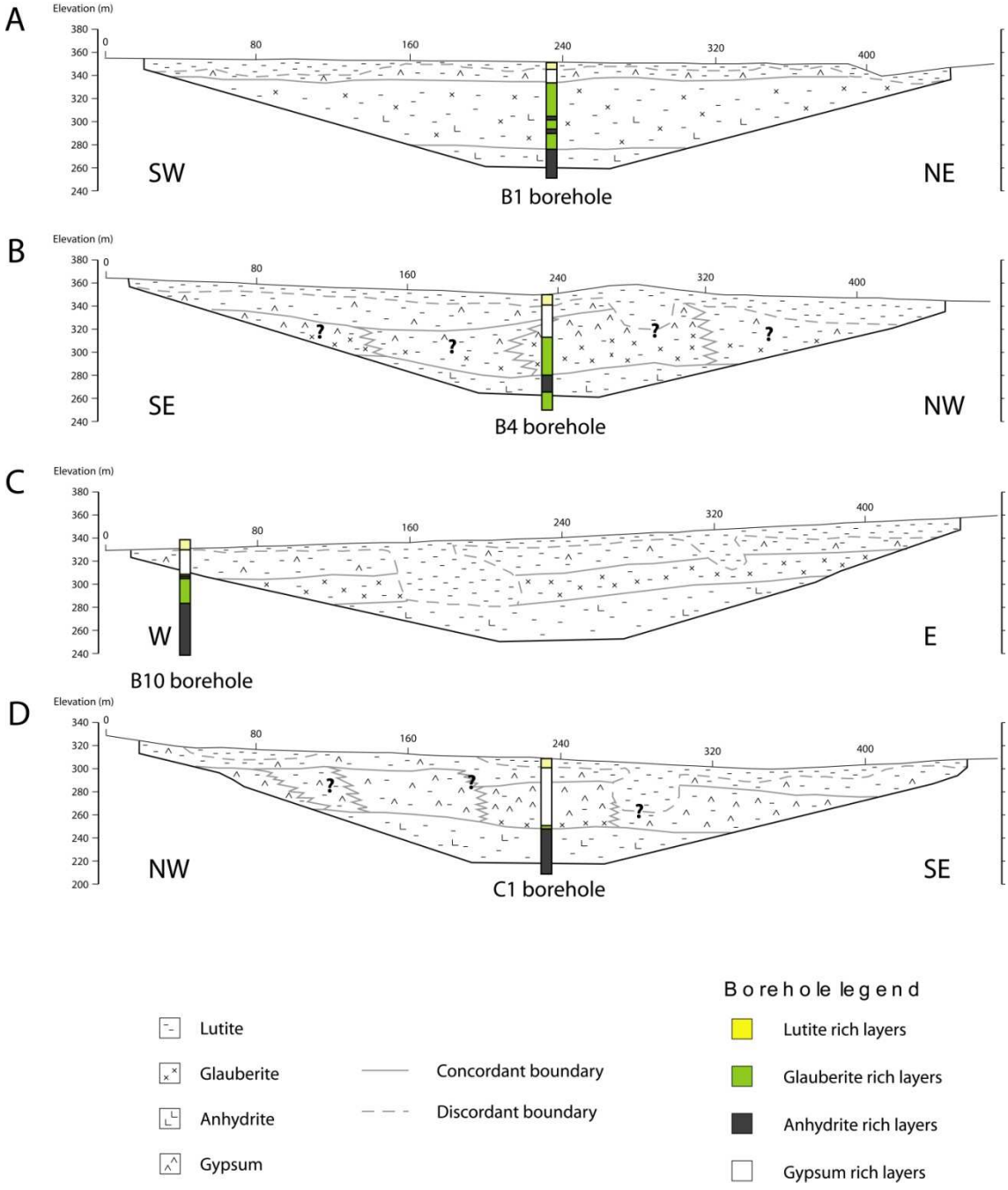

Figure 4.33: Geological interpretation of the ERT profiles showed in figure 4.32. The proportion between sulphates and lutite indicate the purity of the materials. The question marks indicate areas in which the interpretation is uncertain. The situation of the profiles is showed in figure 4.29A.

The B10 resistivity section was performed in a dry stream of a creek. The resistivity section (figure 4.32C), is similar to the one of profile B. There are three layers of low resistivity and the one in the middle is more resistive and discontinuous. In this case, the discontinuity of the most pure layer has sharp-vertical bounds instead of progressive ones as in profile B; so probably there have been dissolution processes and infilling affecting the area related to the creek (figure 4.33.C). The depth of the layer with transitional resistivity value fits with the depth of glauberite levels observed in the B10 borehole.

The area of C1 borehole is covered by vegetation, so there are not outcropping rocks. The area is various kilometers far from the other three studied boreholes, so it is expectable to obtain differences with the rest of the profiles. The inverted resistivity section (figure 4.32D) shows a complex distribution of the terrain with both lateral and vertical discontinuities. There are a lot of transitional values meaning that the purity of sulphate in the area is larger than in the cases studied before. In the center of the profile at a depth of approximately 20 meters, there is a local increasing on the resistivity of the deposit. The resistivity reaches values of pure rocks. In the C1 borehole it is observed a quite pure sequence with some relatively thin clayly levels interlayered. The purity of the sulphate rocks seems to decrease at the bottom of the profile when they change from gypsum and glauberitic to anhydritic layers, as it is observed in the C1 borehole (figure 4.33D).

In general, the evaporitical sequence of the Montes de Torrero area has a very impure composition. Thus, from a geoelectrical point of view the rocks are generally percolant and therefore their resistivity values are low. Locally the purity can be higher but without continuity. Being the matrix the conductivity dominating phase, there is no way of differentiating glauberite from gypsum or anhydrite. Because of that, electrical imaging is useful to observe the distribution of the terrain and identify areas with larger purity, but parametric boreholes are necessary for a suitable interpretation of the profiles. Concerning the complexity of the deposits, at this scale (almost 500 meter long profiles with an investigation depth of 90 meter) the compositional variations of sulphate rocks are common.

Additionally to the survey in Montes de Torrero, another formation has been studied in Arrúbal-Alcanadre area (La Rioja). The Ebro River has eroded the Paleocene and nowadays the remaining materials form a cliff in the south part of the quaternary basin. In this cliff outcrops the horizontal evaporitical sequence of the Paleocene in which is possible to observe the layering. Additionally to the information that can be obtained from the cliff materials, some boreholes were performed upon Paleocene nearby (boreholes R1, R2 and A1; their

position is displayed in figure 4.29B). In those boreholes glauberite rich layers were found at different depth. In the three of them the top of a glauberitic sequence has been identified at the topographical height of approximately 330 meters (figure 4.34), but with different compositions.

Regarding to the rocks outcropping on the cliff, there is a 5 meter thick unusually pure layer of glauberite. Due to its purity, the layer is very white and can be easily identified (figure 4.35C). This layer is laterally wedged towards east (figure 4.35B). Towards west there are eroded materials covering the outcrop so it is impossible to know the lateral continuity in that direction, but it probably disappears in the same way that it does in the east; forming a lens. Samples have been taken from the pure glauberite layer in order to measure the quantity of insoluble matrix and purity above 95% in sulphate has been measured. The outcropping glauberite has hydrated and become into gypsum due to weathering; but the calcium sulphate is unaltered at few centimeters depth from the surface.

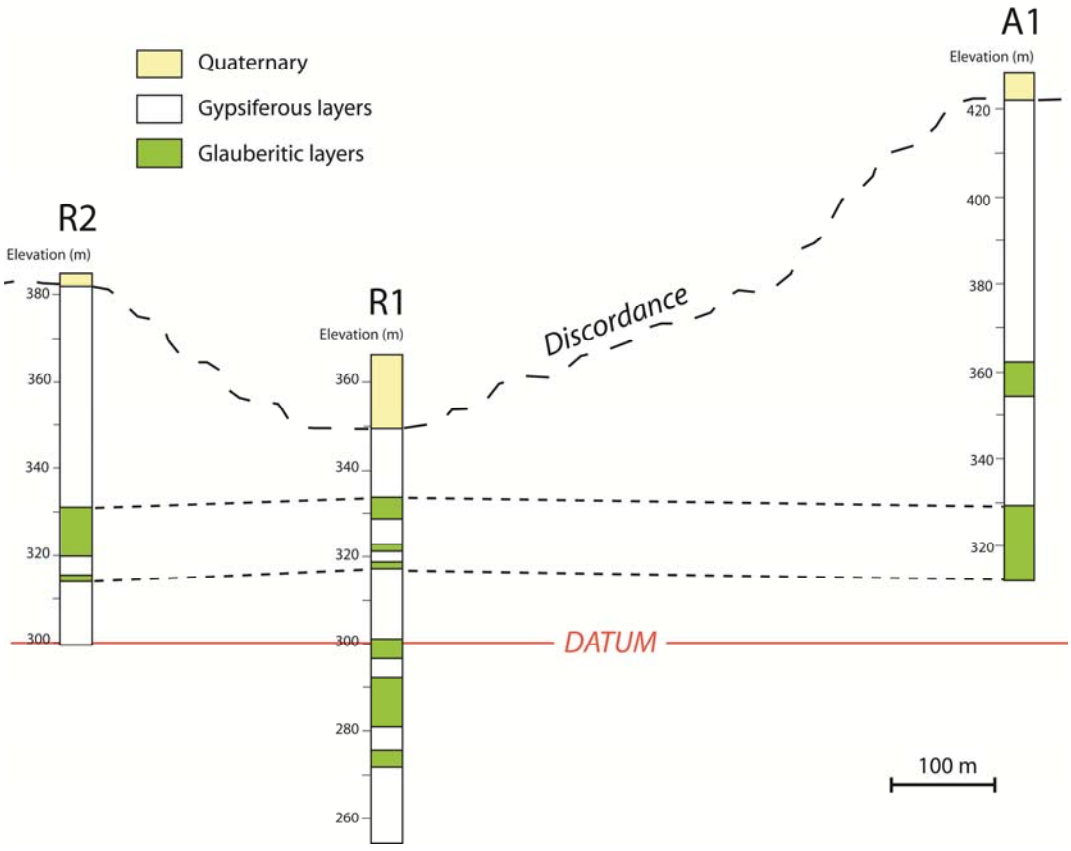

Figure 4.34: Synthetic representation of the boreholes A1, R1 and R2 in the Arrúbal-Alcanadre (La Rioja) area. The possible correlation between layers is marked with dashed lines. The situation of the boreholes is displayed in figure 4.29B. The correlation of the logs has been made with the topographic elevation.

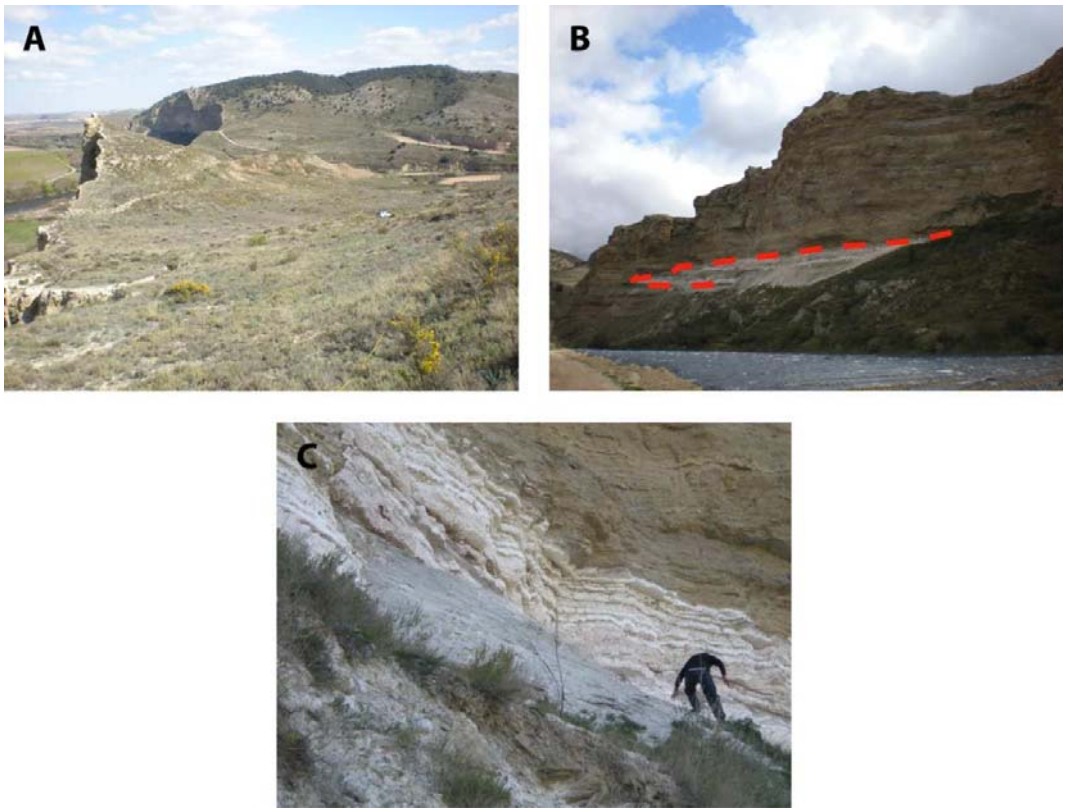

Figure 4.35: Photographs of studied materials in Arrúbal-Alcanadre area. A) South part of the cliff (the cliff is showed at the left of the image) in which A profile was spread; B) General view of the evaporitical materials conforming the cliff; the glauberite layer is marked with a red dashed line; C) Detailed view of the glauberite rocks in which the layering can be appreciated.

The geoelectrical survey has been performed in the south part of the Ebro River, in the upper part of the cliff (figure 4.35A). Two ERT profiles have been performed with the aim of identifying the pure glauberite deposit observed in the cliff and define the electrical resistivity value of glauberite in non-percolant matrix conditions. The profile A has been performed parallel to the cliff and the profile B, obliquely (figure 4.29B). In the cliff, the glauberite layer is below an impure gypsum sequence of approximately 20 meters, but in the area in which the profiles have been spread, there is a topographic depression; so the depth of the layer from the surface is at approximately 12 meters. Below, as it is observed in the east part of the cliff, the rocks are formed of impure gypsum similarly to the upper part.

In the inverted section of profile A (figure 4.36A), a heterogeneous distribution of the resistivity is showed. The section observed in the cliff, corresponds with the horizontal stretch of 100-200 meters. The shallowest low resistivity layer is generated by the low purity gypsum rocks; whose lutitic matrix is percolant. Below the impure gypsum, the resistivity increases

achieving values up to 2500 ohm.m in rectangular-shaped bodies. In the part of the profile which coincides with the cliff situation, there is one of those resistive bodies at the depth in which the pure glauberite layer is; so the body of the SE probably also corresponds with a similar deposit. The lack of lateral continuity of the glauberite layer has been observed in the cliff as well as in the resistivity section. The thickness of the glauberite layer is exaggerated in the inverted profile. Below the resistive layers, Wenner-Schlumberger array tends to create resistive shadows due to decreasing of the sensitivity related to the presence of the resistive materials. Dipole-Dipole array was also tried but the data ser was distorted due to the proximity of the cliff. At the bottom of the profile the resistivity decreases because of the purity decreasing of the sulphates.

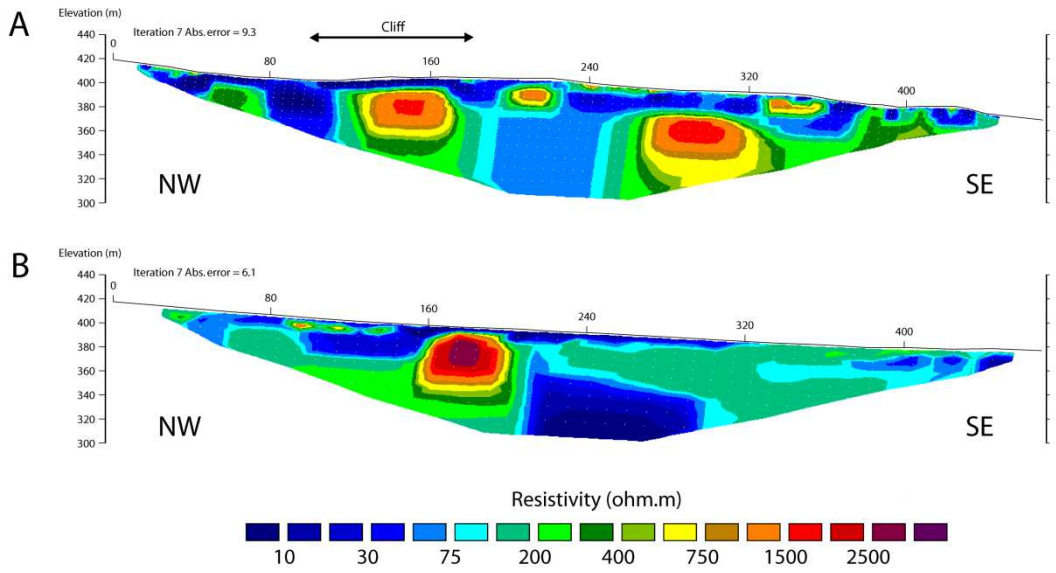

Figure 4.36: Inverted resistivity images of Arrúbal-Alcanadre area. The position of the cliff (parallel to the profile) is marked with a black arrow in the profile A. The situation of the profiles is showed in figure 4.29B.

The profile B (figure 4.36B) displays a similar resistivity distribution of the terrain. In this case the glauberite layer observed in the cliff is also showed as a resistive body (up to 3000 ohm.m) in the NW part of the profile. This section of the layer is just some meters towards south from the one observed in profile A. In the SW part of the profile (which is the furthest one from profile A) there is not any resistive body, but the sulphate layers display transitional resistivity values (>100 ohm.m); this means that the purity is above 55% in sulphates for that area. As it has been showed in the boreholes, there probably are some other glauberite layers

at different depths which are not identified with the electrical imaging due to their lower purity.

In Arrúbal-Alcanadre, a great complexity of the resistivity distribution of the terrain has been shown as in the profiles of Montes de Torrero area. The purity of the glauberite layer showed and sampled in the cliff is very unusual and in most cases the glauberite is mixed with large quantity of lutitic matrix due to its depositional environment. Thus, the deposits of Montes the Torrero are more representatives of a typical glauberite deposit as general trend. This means that normally glauberite rocks are in the percolating matrix domain of the resistivity range of sulphate rocks and there it is not possible to identify them only with geoelectrical methods; there is need of additional information as boreholes.

.3.4 Geoelectrical classification of glauberite rocks

As it has been shown before, glauberite rocks bear different sulphate phases besides the matrix component. In this section it will be considered that the sulphate component is made of a combination of gypsum, anhydrite and glauberite, though other evaporitical minerals as thenardite (Na_2SO_4) or chlorides may be present. The percolation phenomena described in the cases of gypsum and anhydrite rocks has been also observed for glauberite rocks. Therefore it is expectable to obtain the resistivity trend of lower Hashin-Shtrikman bound to compositions within the matrix-percolation zone (purity of 55% or below), while within the sulphates dominant zone (purity of 70% or above) it will fit to the upper bound. Between these two dominium there is a transitional zone in which the resistivity values do not fit to the HS bounds.

It is possible to calculate the HS bounds for a 4-phase system from the general formulae given by Berriman (1995) for n-phases, but this system is much complex than the case of three phases and usually simplifications are used (Torquato 2002). Furthermore, the representation of this 4-phase system is tetrahedral, which is hard to be used. In any case, as it has been showed for the case of anhydrite, the sulphate rocks in the matrix percolation zone have the same resistivity trend for any combination of sulphate because they act as resistances. Thence, for rocks with less than 55% in sulphate purity, a binary system sulphate-matrix can be considered. The lower HS bounds of glauberite-matrix, anhydrite-matrix and gypsum-matrix have been calculated to show that there are not significant differences (figure 4.37). The resistivity value selected for the case for pure glauberite has been 3000 ohm.m,

which is the one calculated for the pure glauberite layer studied in La Rioja. The exactitude of this value is not important as it will be discussed later. For the anhydrite and gypsum phases 10^4 and 10^3 ohm.m respectively has been selected; as in previous sections. In the transitional zone (purity between 55 and 70% in sulphates), the obtained values should be between the HS^- and HS^+; depending of the composition for each case (figure 4.37).

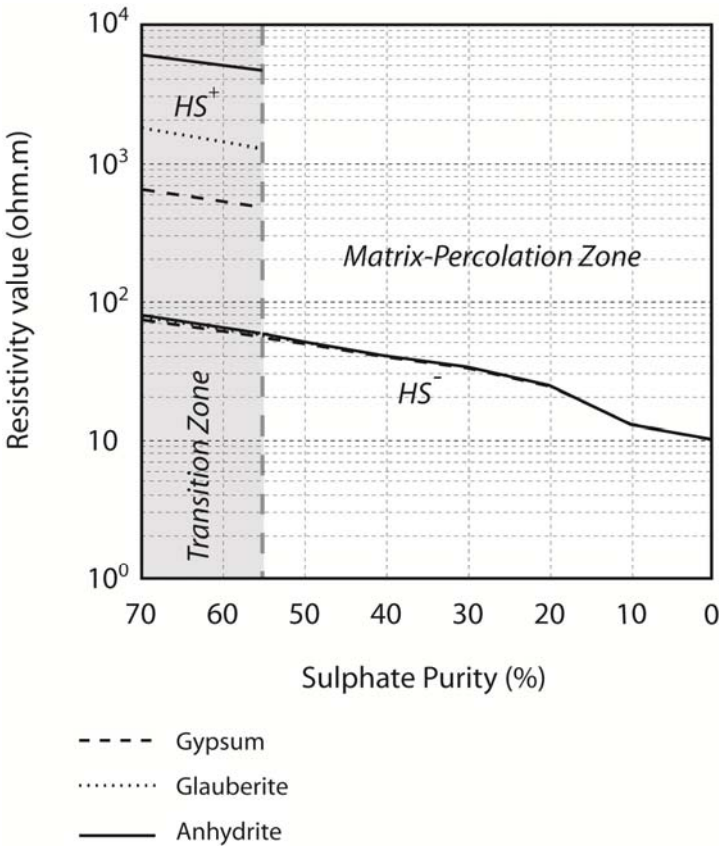

Figure 4.37: Hashin-Shtrikman lower bounds (HS^-) for two phase systems (sulphate and matrix). In the transition zone where the percolation of the matrix ends, the upper bounds (HS^+) are also displayed. The lower bounds for any sulphate-matrix combination within the matrix-percolation zone have the same resistivity trend. Purities in sulphate above 70% are not represented.

In the case of the glauberite rocks with a composition above 70% in sulphate purity, the matrix is no percolant and therefore the dominant phases are the sulphate ones. The representation of these compositions has been by means of different ternary diagrams in which glauberite, anhydrite and gypsum compositions are displayed for a constant matrix quantity for each diagram (30%, 20%, 10% and 0% respectively; figure 4.38). Each ternary diagram represents a 100%; but this 100% only corresponds to the sulphate phases, this is, the

70, 80, 90 or 100% of the bulk rock for each case. These diagrams have been calculated as the HS^+ of 3-phase systems (glauberite, anhydrite and gypsum) alike the case of anhydrite rocks classification (figure 4.27). The corner values have been calculated as the HS^+ of the correspondent sulphate (pure) for a 2-phase system (matrix-sulphate) with 30, 20, 10 and 0% of matrix for diagrams A, B, C and D respectively.

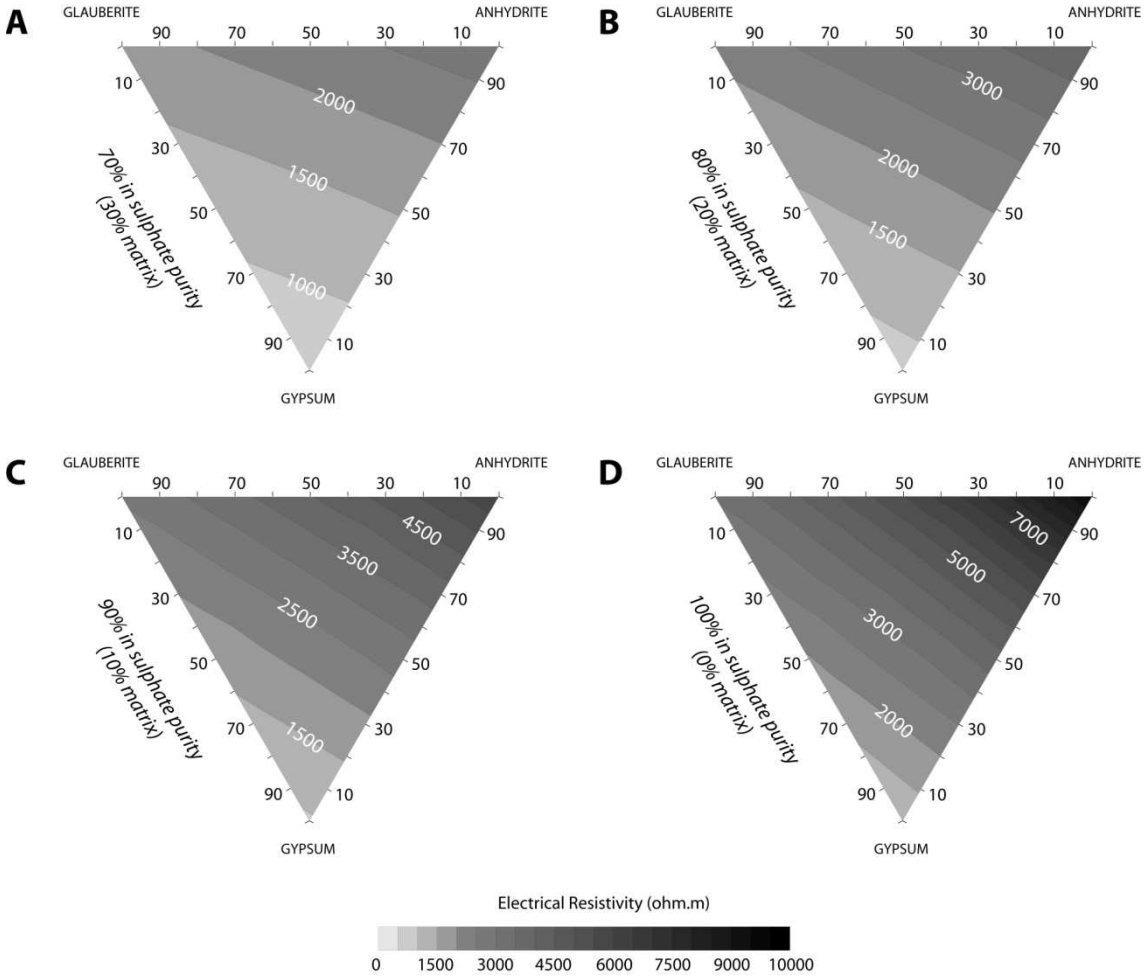

Figure 4.38: Hashin-Shtrikman upper bounds for purities in sulphates of 70% and above (within the sulphate dominium) in the case of the 4-phase glauberite-anhydrite-gypsum-matrix system. The representation is displayed as 3-phase systems with different constant quantities of matrix (30%, 20%, 10% and 0%).

These diagrams show that unlike the matrix-percolation zone, in the sulphate dominant zone the quantity of each sulphate component has a direct influence in the resistivity of the rock. The trend of the resistivity is similar for any matrix composition (considering 30% or below), being the anhydrite the most influent phase. The main difference between them is that in general the resistivity increases as the matrix composition decreases.

The resistivity gradient is also increased in the case of the diagrams with the purest compositions in sulphates. The resistivity values observed in the diagrams overlap for a lot of different compositions. Therefore, is possible to foresee the theoretical resistivity which a glauberite rock of a certain composition will display, but it not possible to interpret the composition from a resistivity data set.

As it has been noted at the introduction of this section, there are no references in the bibliography about the electrical properties of glauberite. We have considered that pure glauberite has 3000 ohm.m. This is coherent with the crystallographic laboratory essays performed in section 4.2.3, in which it has been observed that the water component of gypsum makes it more conductive than the anhydrous sulphate phases (1000 ohm.m). In most cases, with geoelectrical techniques is not possible to differentiate between 1000 and 3000 ohm.m unless it is very close to the surface (measuring high apparent resistivity), because they are very similar. In any case, it is very rare to found a pure glauberite layer such as the one observed in Alcanadre (La Rioja); so in most cases the glauberite will be mixed with an important amount of matrix. This means that the glauberite rocks resistivity range will be between 10 and 60 ohm.m for regular cases, and higher values will be bounded to the presence of gypsum, anhydrite and/or other evaporitical minerals.

In general, the calculated diagrams for this section do not provide significant information, but it is interesting to observe the evolution of the complexity of the bulk rock resistivity as more phases are added to the system. In the case of gypsum rocks, a 2-phase simple system has been defined in which is possible to interpret the composition from the resistivity obtained. In the case of anhydrite rocks, anhydrite mineral has been added to the later system and the complexity of it has increased; still it has been possible to obtain compositional information from the resistivity values. For the current case with 4-phase system (or systems with more phases) additional information must be obtained (as boreholes) to the estimation of the rock composition.

.4 POLARIZATION OF SULPHATE ROCKS

Some type of rocks can be polarized by the effect of electrical current running through them. The chargeability of sulphate rocks is not mentioned in the bibliography. This phenomena, has been observed for sulphate rocks in the case of laboratory essays. In the conductivity measuring of gypsum and anhydrite pills (sections 4.1.3 and 4.2.3 respectively), polarization has been showed; but the most polarized samples have been the ones with most quantity of clay in their composition. Samples with less than 40% of matrix have not suffered polarization (figure 4.7). From this, it can be deduced that in the case of the pills, the polarization is bound to the clay (which polarizable nature is previously known) and unrelated to the sulphate phase; but the sulphate of the pills is made of synthetic homogeneous powder with disordered microcrystals.

In the case of the measures in gypsum crystals samples (section 4.2.3), which are composed of pure gypsum, they have shown polarization with time in both main-foliation parallel and perpendicular directions. Compared to the gypsum pills, it seems that the crystalline structure is somehow related to the polarization of the sulphate phase. Additional trials have been performed upon microcrystalline gypsum, anhydrite and glauberite bricks and sheets and polarization has been observed once again. Other materials as limestone, granite or sandstone sheets have been measured and polarization has not been shown.

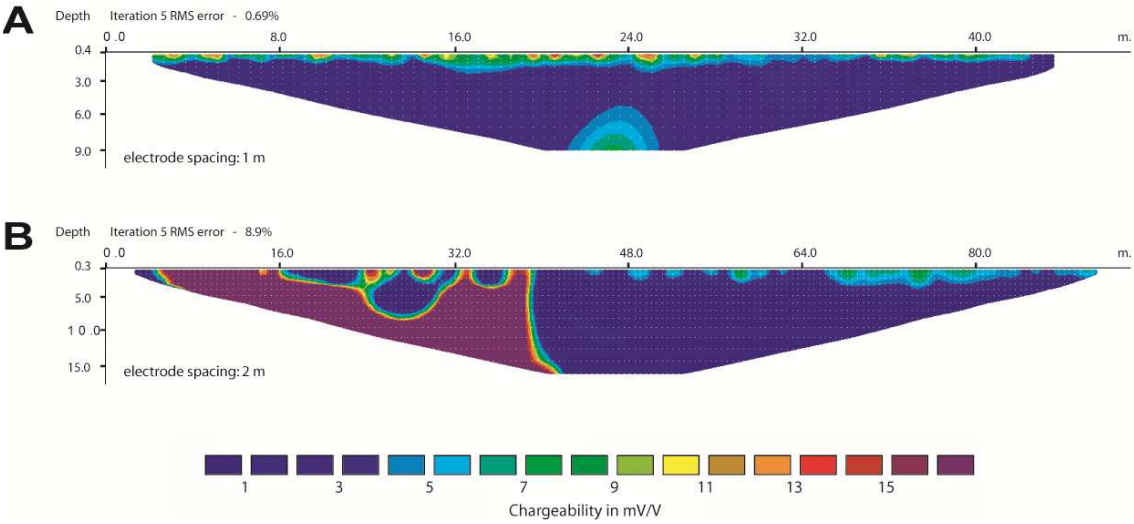

Figure 4.39: Chargeability sections of field examples. A) a terrain with no chargeability anomalies in Cervera; B) chargeability profile with noisy data in Vilobí del Penedès area. Location of the profiles in figure 4.1 (points D and B respectively).

The polarization of sulphate rocks has been studied by means of the induced polarization technique. In some of the sulphate deposits previously studied, chargeability profiles have been elaborated in order to compare the results with the trends observed in laboratory conditions at smaller scale. In some cases the profiles have not shown any chargeability anomaly, but in general the data sets are noisy (figure 4.39). This is due to that the range of the IP measures is very low and it is very sensitive to any source of electricity in the terrain. Only in Pira gypsum formation chargeability has been measured showing some trend coherently in different profiles. In this deposit, the chargeability affects to a gypsum layer with transitional composition (approximately 50% in gypsum purity). The reason of the polarization of the sulphates is unknown and the obtained data is not enough as to extract reliable conclusions. In any case, the IP results of Pira are further explained in chapter 6.1; but the trend obtained is considered as local.